A comparison of 4th and 5th generation thermal networks with energy hub

François, Lédée, Ralph Evins

2024

Original citation:
Lédée, F. Evins, R. (2024) A comparison of 4th and 5th generation thermal networks with energy hub. *Energy* (311). https://doi.org/10.1016/j.energy.2024.133336

Energy 311 (2024) 133336

Contents lists available at ScienceDirect

Energy

journal homepage: www.elsevier.com/locate/energy

A comparison of 4th and 5th generation thermal networks with energy hub

François Lédée *, Ralph Evins

Energy in Cities group, University of Victoria, BC, Canada
Institute for Integrated Energy Systems, University of Victoria, BC, Canada

ARTICLE INFO

Dataset link: https://gitlab.com/fledee/detail_network

Keywords:
District thermal network
Comparison
Heating & cooling
Energy hub
Linear programming

ABSTRACT

State-of-the-art thermal networks are key to address decarbonization of the heating and cooling in buildings. Energy Hub considers synergy between elements and allows rapid comparison between district energy systems incorporating 4th generation (4G) and 5th generation (5G) thermal networks at early-stage designs. To better understand and quantify the differences between systems based on 4G and 5G, a mixed-integer linear model distinguishing specific features of both technologies is implemented. We find systems relying on 5G to perform environmentally and financially better than with 4G generation over a wide set of scenarios. This is due to the warm/cold coupling characterizing 5G technologies. Systems based on 5G can also reduce its carbon emissions more than those with 4G. However, performances with both technologies appear sensitive to the topology and location of central energy station.

1. Introduction

The development of distributed multi-energy systems (MES) has been identified as a key driver in energy transition [1,2]. Most recent developments of district thermal network (DTN) technologies place thermal networks at the heart of the MES concept, by increasing the integrability of renewable energy sources and exploiting low temperature waste-heat.

Currently, two technologies of district thermal networks are considered state-of-the-art [3]: 4th generation (4G) district heating [4] and 5th generation (5G) district heating and cooling [5].

4G networks are centralized systems in line with the three previous generations [6]. Their low operating temperature (50-70 ° C) allows thermal sources such as industrial waste heat, renewable energy and centralized heat-pumps to compete with fossil fuels. They are commonly designed to supply heat, while a cooling service may be planned independently [7] or in parallel [8].

5G networks consist of a warm and a cold pipe with temperatures close to ground temperature (5-30 ° C) [3,5,6,9,10]. In heating mode, heat-pumps (HP) extract heat from the network, and the cooled water is returned to the cold pipe. Water temperature in the building is raised using the extracted heat [9]. The inverse principle is used to deliver cooling, injecting heated water back to the warm pipe. This strong coupling between warm and cold sides induced by the usage of decentralized HP is the essence of 5G networks. This supports electrification, allows the integration of decentralized renewable energy (RnE) and ultra-low temperature waste-heat [3]. Each customer becomes a prosumer [6].

As more technologies can be used to generate thermal energy, the complexity of designing and operating district thermal systems increases [11]. Advanced modeling, e.g. following the "Energy Hub" (EHub) concept [11], were found relevant from early design stages to identify potential synergies between diverse technologies and sources to be exploited [1,11,12]. The EHub concept gathers production, storage, conversion and consumption of different energy carriers within one model, in a unified and interacting fashion [13]. Such model is commonly described through Mixed Integer Linear Programming (MILP) [1] to determine financially or environmentally optimal integration of technologies into a MES [14,15].

Some studies compare 4G and 5G networks, as detailed in the literature section. Those not using the EHub concept omit the synergies between technologies and sources [16–21]. Two of them use the EHub concept [8,22], but fundamental aspects of the 5G network are missing [9] and place the technology at a critical disadvantage. Moreover, current literature is lacking a deeper investigation of the influence of model characteristics on the results. The present study addresses the following questions: (1) What expected differences in design, environmental and financial performances of integrated energy systems result from the consideration of 4G or 5G DTN technology at early design stages? (2) How do key modeling parameters influence the design and performances?

Related literature is presented in Section 2. Section 3 describes the full model. Section 4 covers data, control assumptions, tested network layouts and scenario parameters. Section 5 discusses the study limits. A detailed comparison of base scenarios is presented in Section 6.1.

* Corresponding author.
E-mail address: ledee.francois@gmail.com (F. Lédée).

https://doi.org/10.1016/j.energy.2024.133336
Received 30 August 2023; Received in revised form 6 September 2024; Accepted 30 September 2024
Available online 9 October 2024

Nomenclature

Acronyms

4G/5G	4th/5th generation
AChill	Absorption Chiller
ASHP	Air Source Heat Pump
CHP	Combined Heat and Power
COP	Coefficient of Performance
DTN	District thermal network
EB	Electric Boiler
EChill	Electric Chiller
EHub	Energy Hub
GB	Gas Boiler
HP	Heat Pump
HWT	Hot Water Tank
HX	Heat Exchanger
MES	Multi-energy system
MILP	Mixed Integer Linear Programming
PSO	Particle Swarm Optimization
PTES	Pit Thermal Energy Storage
PV	Photovoltaic
RnE	Renewable Energy
ST	Solar Thermal
WH	Waste Heat
WiP	Water in Pipes

Constants

α^R	Surface per capacity unit
β	Storage limit factor
Δp_x	Max pressure gradient
ΔT	Temperature difference
ΔT^{flex}	Max. T variation of network water
ϵ	width of pipe's house
η	efficiency
η_{lin}	Linearized pumping efficiency
κ	Static storing efficiency
λ	thermal conductivity
ρ	Water density
A_{max}	Max Roof area
C	Price
c_p	Water thermal capacity
D	Diameter of pipes
f_D	Darcy–Weisbach friction factor
G	Carbon intensity
H	conversion efficiency matrix
I^{sun}	Sun irradiation
L	Length of link
M	BigMparameter
NPV	Net Present Value
T_s	Temperature of soil
T_w	Temperature of water
X_{CO_2}	Carbon emission limit

Ensembles

$\sigma \in S$	Set of streams
$\tau \in \mathcal{T}$	Set of technologies or links
Ξ^{Net}	Set of techs if connected
Ξ^{Node}	Set of techs if standalone
$f \in \mathcal{F}$	Set of fuels
$l \in \mathcal{L}$	Set of links
$n \in \mathcal{N}$	Set of nodes
$t \in \mathbb{T}$	Set of time steps

Subscripts/Superscripts

ch	charging
cv	a converter
dch	discharging
fix	Relative to fixed part
$H\ /\ C$	hot/cold
in	entering
lin	Relative to linear part
$load$	power demand/load
out	exiting
ref	main/of reference
s	a storage

Variables

δp	Pseudo-pressure level
δ	binary for installation status
$\dot{Q}$	Thermal power
$\dot{Q}^{\mathcal{L}}$	Power between node and network
$\dot{Q}^{\mathcal{N}}$	Power between node and source
$\dot{q}^{el}$	circulation losses
$\dot{q}^{th}$	thermal losses
J^a_{CAPEX}	Annualized investment cost
J^a_{tot}	Total annualized cost
J_{CO_2}	Cost of carbon taxes
J_{fuel}	Operating cost
$J_{O\&M}$	Cost for maintenance
P_{nom}	Capacity of device
SOC	State of Charge

Sensitivity to the financial and environmental strategy, use of local renewable electricity, and geographical aspect of the model are presented in Sections 6.2–6.4 respectively. Finally, implications and future perspectives are discussed in Section 7.

2. Literature & scope

2.1. Modeling 4G DTN with EHub

Numerous EHub based methodologies have been suggested in the literature to find optimal topologies and technological synergies for 4G networks.

Some methodologies exclusively focus on the topology, with little regards for the technologies to supply energy or the operation. The selection of clients to connect via the DTN is of prime interest and was explored using peak demand [23], including the location and thermal power for central plants [24] and in coupling with the topology of natural gas and power network [25]. The latter concludes on the importance to include network losses in the modeling.

Some methodologies exclusively focus on the central station of 4G networks. The selection, sizing and operation of sets of technologies to ensure the supply is addressed, while geographical spread and selection of customers is excluded. The synergies between dispatchable thermal generation units are evaluated by Kuriyan et al. [26], including neither RnE nor storage. Storing capabilities of the network by variation of the network temperature are assessed in [27], while the benefit of boreholes [28], hydrogen storage [29,30] and a mix long and short-term storage technologies [31] were also studied. The sector coupling is also investigated to evaluate the potential of DTN integration with

local and utility power grids [2], the need for upgrades in electric and heating networks [32] and the benefits of coupling heating and cooling generation in the central station of a 4GDTN [33].

Methods to compare centralized vs. decentralized while investigating synergies between technologies are also suggested. Unternährer et al. [34] select and size dispatchable units of a central station with an EHub model, after a separate optimization of the network topology. Morvaj et al. [35] address both topology and size optimization within one EHub formulation, including storage, RnE and hourly operation of the whole system. The operational aspect was validated against simulations in [36] and used in [37] to address multi-scale planning. Gas network, thermal network and transportation planning are coupled within an EHub by Pantaleo et al. [38,39] to study the integration of biomass in a city.

2.2. Modeling 5G networks

Linear optimization and the EHub concept have been little used for design and operation of 5G systems. Prasanna et al. [40] validate MILP and EHub concepts against data of a real system including borehole. The model is further used to study the potential of additional decentralized storage systems on the self-sufficiency of the whole system. Wirtz et al. [9] suggest a MILP formulation to size and operate all centralized and decentralized supply and storage around an already-designed 5G network for a university campus. The pre-sizing of the network prevents investigating centralized-decentralized trade-offs, the effect of long-term storage and carbon transition.

Linear Programming has been used for modeling 5G networks to study optimal operation strategies as well [40–43]. Although MILP was proven sufficiently accurate for early-stage studies, it is widely considered that fundamentally non-linear characteristics of thermodynamics and fluid mechanics [44] make linear solutions non suitable. Thus, a vast majority of studies rely on simulation models such as TRNSYS [44,45] or Modelica [46,47]. However, these only assume a predefined layout and supply set [10,48–52], compare predefined configurations [53,54], conceive ad-hoc iterative processes [21,55,56] or integrate the simulation into evolutionary algorithms (e.g. PSO [16, 57]). In their review, Brown et al. [44] acknowledge the need for a unified framework encompassing all aspects of the 5G network. Taylor et al. [54] also conclude simulation-based approaches do limit the exploration of trade-offs, synergies between technologies and usage of storage, which justifies the usage of MILP and EHub for early-stage designs of 5G networks.

2.3. Comparison of DTN technologies

A recurring question to address at very early-stage design is the choice of network technology. Transiting from centralized generations 1 to 4, the main concern is the reduction of supply temperature [58], allowing to integrate new energy sources [59–61]. Interacting with a decentralized 5GDTN is fundamentally different [6], and requires two closely related loops (warm and cold). Low temperature sources (waste heat, ground, etc.) and specific dispatchable units regulate the network (central station, borehole, long-term storage, etc.). Therefore, models encompassing specificities of each DTN technologies are needed for comparisons.

Gudmundsson et al. [19] use simulation for an economic comparison of 4G and 5G. They conclude the cheaper operation of 5G does not compensate for the high investment costs. Their method is only applied to heating service for residential districts and does not consider energy generation. Gross et al. [18] use simulation in a district with diversified loads to show the impact of active prosumers on a 5GDTN. They validate their flow model against data. Their method focuses on energy savings and no diversity of energy generation is considered. Jebamalai et al. [20] evaluate financial gains of specific topologies of centralized networks over a 5G network. They find 5G is only preferable if industrial waste heat is available for free. Their method does not consider any choice or design of the supply, and long-term storage is only considered for the centralized networks. Barely any cooling is included in their case study. Calise et al. [17] compare the DTN technologies with TRNSYS models for a residential district. Heating and cooling do not occur simultaneously, which allows the same infrastructure to supply heat in winter and cold in summer with the 4G network. Both networks only rely on an already designed central ground source heat pump, partially fed with 3MWp of solar panels. They conclude on the economic and environmental superiority of mature 4G technology for purely residential districts with little load sharing potential.

Brumana et al. [16] use PSO to design the most cost-effective PV-Battery-Chiller system to support both DTN technologies. They find centralized networks financially advantageous and requiring less generation capacity. Their methodology neglects the heat-cold coupling of the 5GDTN and is only applied to residential buildings. Millar et al. [22] compare financial performances of the two DTN technologies with an EHub. For 4G and 5G, a single pipe at constant temperature connects buildings of different nature. Storage, HP (5G) and exchangers (4G) are sized. They find that with storage, 5G is cheaper than 4G. However, their 5G model neglects the fundamental heat-cold coupling, and only financial performances are assessed. Nérot et al. [8] compare multiple DTN technologies for different objectives and climates with an EHub. The DTN and generators are designed and operated to supply heating and cooling. They find 4G is the best trade-off between financial, environmental and exergy efficiency. 5G performs consistently worse than 4G and is only comparable to buildings operated individually. Their methodology uses a single ambient loop for 5G, with little difference with other generations in the way the network operates. This also neglects the heat-cold coupling. The method is used on a fully residential district, where seasonal storage and RnE is only available for 4G. Zhang et al. [21] combine optimization and simulation for an economic comparison of 4G and 5G. Their method sizes small thermal storages and is used for a mixed set of buildings under multiple electricity price, weather and retrofit scenarios. They find that 5G is not economically viable compared to 4G, unless the cooling share is above 27% or unless the price of electricity drops drastically. Their method does not include selection and sizing of energy generation, does not consider local PV and the analysis does not include carbon emissions.

2.4. Contributions

In this paper, an EHub model is used to compare the economic and environmental performances of MES relying on 4G and 5G DTN in various contexts. The model includes the selection of customers to connect to the network, i.e. the trade-off between connected and stand-alone thermal supply. The comparison is conducted for 3 climate zones in the USA and across a variety of financial and technical scenarios. The main contributions of this paper are:

- comparing overall expected performances of a MES relying on 4G and 5G technologies including all the features mentioned in Table 1.
- investigating the sensitivity of the comparison to strategic model parameters.

3. Methodology

The energy system model is split into nodes (hosting the energy loads, imports, exports and transformations) and a network layout (handling energy transfer between nodes and transmission losses). All model variables, including capacities, operation and energy purchase, are determined collectively via optimization (cost and emissions minimizations) using Gurobi [62]. This section presents the optimization objectives, then the linear formulations for the network and node models.

Table 1
Studies comparing 4G and 5G DTN technologies via modeling.

	Brumana et al. 2022 [16]	Calise et al. 2023 [17]	Gross et al. 2021 [18]	Gudmundsson et al. 2022 [19]	Jebamalai et al. 2022 [20]	Millar et al. 2021 [22]	Nérot et al. 2023 [8]	Zhang et al. 2022 [21]	Current study
Heat & Cold	✓	✓			✓	✓	✓	✓	✓
H&C coupling		✓						✓	✓
min $ & CO_2							✓		✓
Long storage					✓*	✓	✓*		✓
Network	Σ	Σ	Σ	Σ	Σ		H	Σ	H
Load diversity			✓		✓	✓		✓	✓
Supply design	E					H		S	H
With RnE	✓	✓	✓					✓	✓

(*) Not available for 5G.
(Σ) Simulation; (H) Energy Hub MILP.
(E) Evolutionary algorithm; (S) Scenario.

3.1. Objective function of the optimization

The cost J^a_{tot} in Eq. (1) combines OPEX (operational expenditure) and annualized CAPEX (capital expenditure). The CAPEX considers the purchase and installation of the whole system considering prices C and installed capacities P^{nom}, and is annualized (Eq. (2)). The OPEX includes energy bills J_{fuel}, carbon taxes J_{CO_2} and maintenance costs $J_{O\&M}$ and is not annualized. Bills in Eq. (3) and emissions in Eq. (4) consider net purchases of fuel and power $\dot{Q}$, prices, and carbon intensities G for the latter.

$$J^a_{tot} = J^a_{CAPEX} + J_{fuel} + J_{CO_2} + J_{O\&M} \tag{1}$$

$$J^a_{CAPEX} = \sum_{\tau \in \mathcal{T}} NPV_\tau (C^{fix}_\tau + P^{nom}_\tau C^{lin}_\tau) \tag{2}$$

$$J_{fuel} = \sum_{f \in F} C^{fuel}_f \sum_{n \in \mathcal{N}} (\dot{Q}^{\mathcal{N},in}_{n,\sigma_f} - \dot{Q}^{\mathcal{N},out}_{n,\sigma_f}) \tag{3}$$

$$J_{CO_2} = C^{CO_2} \sum_{f \in F} G_f \sum_{n \in \mathcal{N}} (\dot{Q}^{\mathcal{N},in}_{n,\sigma_f} - \dot{Q}^{\mathcal{N},out}_{n,\sigma_f}) \tag{4}$$

A carbon-cost optimal front is computed using the epsilon-constraint method [63] to simulate a forced decarbonization.

$$\sum_{f \in F} G_f \sum_{n \in \mathcal{N}} (\dot{Q}^{\mathcal{N},in}_{n,\sigma_f} - \dot{Q}^{\mathcal{N},out}_{n,\sigma_f}) \leq X_{CO_2} \tag{5}$$

3.2. Network model

The model is tailored for very early design explorations. For the model to remain linear and tractable [42], a purely energy-based approach is considered, inspired by [35]. The model assumes a predefined and homogeneous temperature difference ΔT, and assumes water massflow $\dot{m}$ to be only influenced by pressure control [9]. The temperature difference is the difference between warm and cold pipes in the 5G network and the difference between supply and return in the 4G models. This results in a direct link between transferred thermal power $\dot{Q}$ and mass flow control (Eq. (6)), allowing to only consider the transferred power as model variable. The modeling of thermal and circulation losses is revised consequently.

$$\dot{Q} = \dot{m}\ c_p\ \Delta T \tag{6}$$

3.2.1. Interface between nodes and network

The network can transfer energy between nodes. A node may take ($\dot{Q}^{\mathcal{N},in}$) or feed energy ($\dot{Q}^{\mathcal{N},out}$) directly to the grid. This energy may reach ($\dot{Q}^{\mathcal{L},in}$) or leave ($\dot{Q}^{\mathcal{L},out}$) the node proximity by any connected link $l \in \mathcal{L}$. Each link may transfer energy in one (4G) or both (5G) directions. Thermal losses $\dot{q}^{th}$ are unrelated to the energy flow in links, while the circulation loss $\dot{q}^{el}$ is positive regardless of the direction of the flow in the pipe. Thus, the interface between each node n and the network for stream σ at all time t is represented via Eq. (7) and Fig. 1a.

$$\dot{Q}^{\mathcal{N},out}_{n,\sigma,t} + \sum_{l \in \mathcal{L}(n)} \dot{Q}^{\mathcal{L},out}_{l,\sigma,t} = \dot{Q}^{\mathcal{N},in}_{n,\sigma,t} + \sum_{l \in \mathcal{L}(n)} \dot{Q}^{\mathcal{L},in}_{l,\sigma,t} + \sum_{l \in \mathcal{L}(n)} \dot{q}^{th}_{l,\sigma,t} \tag{7}$$

3.2.2. Thermal losses in links

5%–15% of the transferred energy is dissipated in the ground due to the temperature difference with the network water [64]. These losses follow Eq. (8) when the pipe l is installed (binary variable $\delta_l = 1$), even if no energy is transferred (unlike most related literature). Polyethylene pipes are uninsulated for 5GDTN ($\lambda = 0.4$ W/m.K) [9,65] and insulated for the 4GDTN ($\lambda = 0.04$ W/m.K) [66]. The term $\dot{q}^{flex}_{l,t}$ refers to an additional thermal loss related to the thermal inertia of a 5G network (see Eq. (21)).

$$\dot{q}^{th}_{l,\sigma,t} = L_l\ \delta_l\ \frac{2\pi\lambda}{ln(1+\frac{2\epsilon}{D})}(T_w - T_s) + \dot{q}^{flex}_{l,\sigma,t} \tag{8}$$

3.2.3. Circulation losses in links

The formulation for the circulation losses in Eq. (9) is adapted to the current energy transfer model and linearized. Since most related studies neglect pumping requirements, no equivalent formulation was found.

$$\dot{q}^{el}_{l,\sigma,t} = \dot{Q}_{l,\sigma,t} \times \left(\frac{8 f_D}{(\rho\pi)^2} \frac{L_l}{D_l^5} \frac{1}{c_p\ \Delta T\ \eta_{lin}} \right) \tag{9}$$

3.2.4. Flows in water pipes

If the network contains cycles,[1] unrealistic loops of energy circulation can bias the model or be exploited to waste energy (e.g. excess of solar renewable) [32]. Thus, an additional variable $\delta p_{n,\sigma}$ is added for each node n and transferred stream σ, resulting in Eq. (10) [35,67]. It can be assimilated to a pressure level, forcing the flow to be unidirectional in pipes at any time t and to never close a circuit.

$$\dot{Q}^{\mathcal{L}}_{l,\sigma,t} = \frac{\tilde{P}^{nom}_l}{\Delta p_x\ L_l} (\delta p_{n_{in},\sigma,t} - \delta p_{n_{out},\sigma,t}) \tag{10}$$

3.3. Nodes

Nodes are where energy is purchased, consumed, produced, transformed and fed in, following the energy hub concept [11,14].

3.3.1. Stream balance

The node is divided into energy streams, each one must be balanced between generation, consumption, storage interactions, imports and exports.

$$\dot{Q}^{load}_{n,\sigma,t} = \sum_{\tau_{cv} \in \mathcal{T}_{cv}} (H_{\tau_{cv},\sigma}\ \dot{Q}^{\mathcal{T},in}_{n,\tau_{cv},t}) + \dot{Q}^{\mathcal{N},in}_{n,\sigma,t} - \dot{Q}^{\mathcal{N},out}_{n,\sigma,t} + \sum_{\tau_s\ on\ \sigma} (\eta^{dch}_{\tau_s} \dot{Q}^{dch}_{n,\sigma,\tau_s,t} - \eta^{ch}_{\tau_s} \dot{Q}^{ch}_{n,\sigma,\tau_s,t}) \tag{11}$$

[1] https://en.wikipedia.org/wiki/Cycle_(graph_theory)

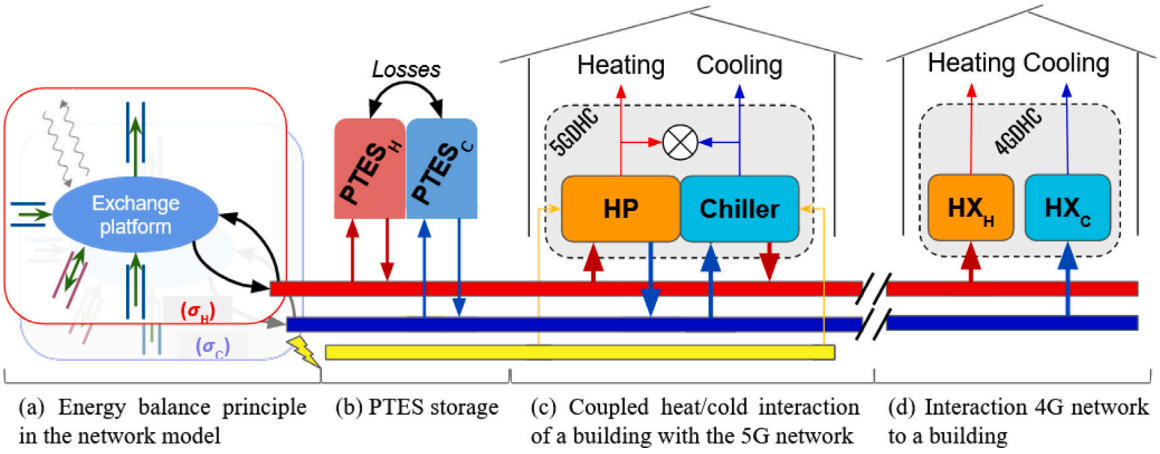

Fig. 1. Visual principles of the models.

3.3.2. Converters

A converter τ_{cv} transforms power from one or multiple streams into one or multiple others. All converters are considered linear. This is common for most technologies (e.g. Boilers, HP, PV, ST) [9,63,68–71]. CHP and Absorption Chillers (AChill) [68,70] are also assumed linear, as a minimum partial load does not influence the system design and partial load efficiency makes the model intractable [71].

A matrix-based formulation describes the operation (Eq. (12)). The unitless coefficient $H_{(\tau_{cv},\sigma)}$ binds each converter τ_{cv} to each stream σ. For HP, solar thermal (ST) collectors and photovoltaic (PV) panels, this coefficient is precomputed for every time step t, it is constant for other converters (c.f. Appendix A). It is negative for inputs and positive for outputs. A reference input stream σ_{ref} is used to determine other input and output powers of each converter τ_{cv} (Eq. (11)). Roof technologies (PV and ST) cannot be curtailed and must convert all received irradiation; a transformed factor $\xi^{roof}_{n,\tau_{cv},t}$ (in kW/kWp) is precomputed to account for direct and diffuse irradiation, air temperature, tilt and orientation [72].

$$\begin{cases} 0 \leq H_{(\tau_{cv},\sigma_{ref})}\ \dot{Q}^{\mathcal{T},in}_{n,\tau_{cv},t} \leq P^{nom}_{n,\tau_{cv}}, \\ \qquad \text{if } \tau_{cv} \text{ is dispatchable} \\ H_{(\tau_{cv},\sigma_{ref})}\ \dot{Q}^{\mathcal{T},in}_{n,\tau_{cv},t} = \xi^{sun}_{n,\tau_{cv},t}\ P^{nom}_{n,\tau_{cv}}, \\ \qquad \text{if } \tau_{cv} \in \{PV, ST\} \end{cases} \tag{12}$$

Every node has a limited rooftop area A^{max} to be shared between PV and ST. This further constrains the capacity of solar techs to be installed, with an assumption of $\alpha^R_{ST} = 2m^2/kWp_{th}$ for ST and $\alpha^R_{PV} = 8m^2/kWp_{el}$ for PV.

$$\sum_{\tau_{cv}\in\{ST,PV\}} \alpha^R_{\tau_{cv}}\ P^{nom}_{n,\tau_{cv}} \leq A^{max}_n \tag{13}$$

A pair HP-electric chiller is used to interact with a 5G network. We call electric chiller (EChill) a HP designed for cooling purposes. Both converters operate independently and interact with both the warm and cold network pipes (Fig. 1c). A third converter helps feeding energy back to the network by cancelling out one unit of active heat with one of active cold within the node (i.e. the demand remains unchanged). This ensures the coupling between warm and cold sides of the 5G network [9,18,73,74] and the connection between heat and cold within a node [9] (c.f. Appendix B).

3.3.3. Storage technologies

The storages link time steps and displace productions to better match the demand. Four storage technologies are considered: HWT, Solar Tank, Water in pipes (WiP) and Pit thermal energy storage (PTES).

The model describes a yearly cycle, thus the State Of Charge (SOC) at the start and end must be identical for every storage (Eq. (14)).

$$SOC_{n,\sigma,\tau_s,\ t^{max}+1} = SOC_{n,\sigma,\tau_s,\ t=0} \tag{14}$$

For the sake of simplicity, the maximum charging and discharging power of every storage is set proportional to its capacity (Eq. (15)–(16)).

$$0 \leq \dot{Q}^{ch}_{n,\sigma,\tau_s,t} \leq \beta^{ch}_{\tau_s} \times P^{nom}_{n,\tau_s} \tag{15}$$

$$0 \leq \dot{Q}^{dch}_{n,\sigma,\tau_s,t} \leq \beta^{dch}_{\tau_s} \times P^{nom}_{n,\tau_s} \tag{16}$$

The capacity of every storage binds the state of charge. For HWT, Solar Tank and PTES, these bounds are depicted by Eq. (17). For the WiP, Eq. (20) is used.

$$0 \leq SOC_{n,\sigma,\tau_s,t} \leq P^{nom}_{n,\tau_s} \tag{17}$$

The time coupling equations are expressed as follows (Eq. (18)) for all but the PTES, and via Eq. (22) for PTES. Decay κ, charging η^{ch} and discharging η^{dch} efficiencies are considered.

$$SOC_{n,\sigma,\tau_s,t+1} = (1-\kappa_{\tau_s})SOC_{n,\sigma,\tau_s,t} + \eta^{ch}_{\tau_s}\dot{Q}^{ch}_{n,\sigma,\tau_s,t} - \frac{1}{\eta^{dch}_{\tau_s}}\dot{Q}^{dch}_{n,\sigma,\tau_s,t} \forall \tau_s \in \{HWT, ST, WiP\} \tag{18}$$

The water in 5G networks has thermal inertia [48,51,74]. This inertia is modeled via another storage whose capacity is defined by the volume of water in pipes (Eq. (19)). Its SOC represents the difference between the expected fixed temperature and the actual temperature in the pipes (Eq. (20)). The resulting additional thermal losses are assessed in Eq. (21) and added to the total thermal losses in Eq. (8).

$$P^{nom}_{WiP} = \rho c_p \Delta T^{flex} \sum_{l\in\mathcal{L}} \delta_l L_l \frac{\pi D_l^2}{4} \tag{19}$$

$$-P^{nom}_{WiP} \leq SOC_{WiP,t} \leq +P^{nom}_{WiP} \tag{20}$$

$$\dot{q}^{flex}_{\sigma,t} = \frac{8\lambda}{\rho c_p \epsilon} SOC_{\sigma,WiP,t} \tag{21}$$

Long-term storage is commonly associated with 5G networks [3,28–30,75]. The PTES technology is chosen for its competitiveness, independence of geological conditions [75] and temperature adequacy [45]. Eq. (22) enforces the time coupling for PTES. Similar model formulations are used in related literature for aquifer and boreholes, coupled with additional HPs for the temperature adequacy [40]. With higher

investment, operating and maintenance costs, other long-term storages would be less accepted. The PTES serves both the warm and cold network sides (Fig. 1b), following principles described in [76,77].

$$SOC_{\tau_s,t+1} = (1-\kappa_{\tau_s})SOC_{\tau_s,t} + \kappa_{\tau'_s} SOC_{\tau'_s,t} + \eta^{ch}_{\tau_s} Q^{ch}_{\tau_s,t} - \frac{1}{\eta^{dch}_{\tau_s}} Q^{dch}_{\tau_s,t} \ \forall (\tau_s, \tau'_s) \in \{PTES_H, PTES_C\}\ ,\ \tau_s \neq \tau'_s \quad (22)$$

3.3.4. Sets of technologies

This work compares DTNs, but nodes can choose to disconnect from it. Specific technologies tailored for collective systems cannot be used by disconnected nodes [34]. In the model, sets of technologies are allowed Ξ^{Net}_n or disallowed Ξ^{Node}_n if a node n connects to any potential link $l \in \mathcal{L}^{(>n)}$ of the DTN. Eq. (23)–(24) links the connection status (binary variable δ_l) with the technology installation status δ_{tau} via the Big$M$ method,[2] M being an arbitrarily large number. The technology sets are described in Section 4.

$$\sum_{\tau \in \Xi^{Node}_n} \delta_\tau \leq M \sum_{l \in \mathcal{L}^{(>n)}} \delta_l \quad (23)$$

$$\sum_{\tau \in \Xi^{Net}_n} (1-\delta_\tau) \leq M \sum_{l \in \mathcal{L}^{(>n)}} \delta_l \quad (24)$$

Table 2
Scenarios and associated values.

	Field	Values	
Always	**Location**	{LA, OR, WI}	
	Generation	{4, 5}	
	CO_2 Reduc	{−0,−25,−50,−75}	%
Strategy	Price Elec	{**0.2**,0.3,0.4}	$/kWh
	Carbon Elec	{**0.25**,0.4,0.7}	$kgCO_2$/kWh
	Carbon Tax	{0,**65**,170}	$/$tCO_2$
	Lifetime	{7,15,**tech**}	y
Resource	Storage	**y**/n	
	MicroGrid	y/**n**	
	WasteHeat	**y**/n	
	Roof Fraction	{ **50** }	%
Layout	Shape	{**Star**, Line, Loop} (Fig. 2)	
	Station	{**Hospital**, SuperMarket, LargeOffice}	

4. Case study

4.1. Scenarios and sensitivity

We name *base cases* the scenarios using exclusively default **bolded** values in Table 2. Alternative scenarios always only use a single non-default value at a time.

Three US locations are selected: Louisiana (LA), Oregon (OR) and Wisconsin (WI) respectively for their hot, temperate and cold climate (Table 3). The carbon reduction is relative to what is achievable. It is not an absolute emission reduction, as outlined in the results section. The value *tech* for the lifetime means the annualization factor is considered for the lifetime of each technology. The roof fraction is the usable fraction of roof surface to install ST or PV. Three of the four load types (hospital, offices, supermarket, residential) are considered to host the central station (c.f. Fig. 3).

4.2. Resources and data

The study uses aggregated cooling and heating loads, where the latter merges demands for hot water and space heating together. Load data of 4 building types over 3 locations (Table 4, Appendix C) from the dataset [78] is used. The dataset is built from EnergyPlus simulations of archetypes in the US.

Table 3
Degree days (base 18.3 °C).

	LA	OR	WI
HDD	754	2326	4082
CDD	1547	204	303

Table 4
Total thermal load for each node.

	LA		OR		WI	
(GWh/y)	Heat	Cold	Heat	Cold	Heat	Cold
Apartments	1.83	5.57	3.39	1.20	6.24	1.53
Hospital	1.38	7.36	1.89	5.26	2.10	5.03
Offices	0.39	6.89	0.68	2.12	1.72	2.37
Superstore	0.44	0.52	1.37	0.04	1.96	0.09

The EnergyPlus website[3] hosts the TMY3 weather files used for the simulations. These files are combined with Gsee[4] (PV) and the model from [79] (ST) to precompute solar resources. They are combined with a model from [80] for the soil temperature and with a model from [81] to precompute the COP of HPs and chillers.

4.3. Temperature setpoints assumptions and waste heat

The water in 5G networks is maintained at 25 °C and 10 °C for the warm and cold sides [6,82]. For the 4G, heat supply and return are at 70 °C and 40 °C [35], cold supply and return are at 6 °C and 12 °C [7]. Demands for hot water and space heating are merged. Heating service is at 40 °C, cooling service is at 12 °C. HP and chiller efficiencies are precomputed for a refrigerant 15 °C above heating service and at 1.7 °C for cooling service. Indoor setpoints are specified in the dataset manual [78].

Waste heat (WH) is modeled by installing additional ST at the central station, inspired by the prosumer model in [18]. The ST capacity used for WH equals half the peak load of the station node. WH only represents a heat production surplus between 60 °C and 80 °C, it has neither investment costs nor roof area, and no associated solar tank.

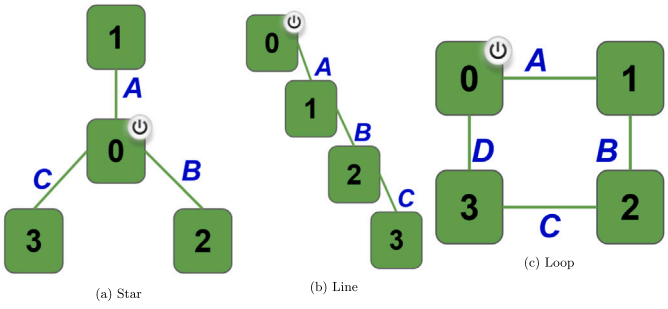

(a) Star (b) Line (c) Loop

Fig. 2. Network configuration layouts.

4.4. System potential designs

4.4.1. Network layouts

Nodes may connect following the "Star" configuration in the base cases (Fig. 2). The interest of "Line" and "Loop" configurations are investigated for the assessment of geographical features in Section 6.4.

[2] https://en.wikipedia.org/wiki/Big_M_method

[3] https://energyplus.net/weather

[4] https://pypi.org/project/gsee/

4.4.2. Nodes layouts

The potential configurations of nodes are shown in Figs. 3(a)–3(c) for 4G nodes and in Fig. 3(d) for 5G nodes. Technologies in black cells are only available for the central station. If a central station disconnects from the network, then:

- 4G: the potential layout of the central node becomes identical to those of a regular node (Fig. 3(a))
- 5G: elements in black cells in Fig. 3(d) are no longer available.

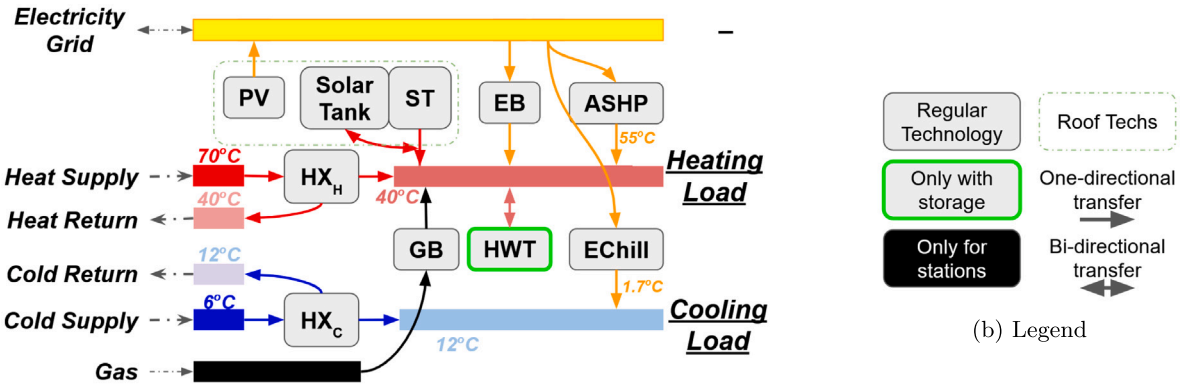

(a) Potential node connected to a 4G network

(b) Legend

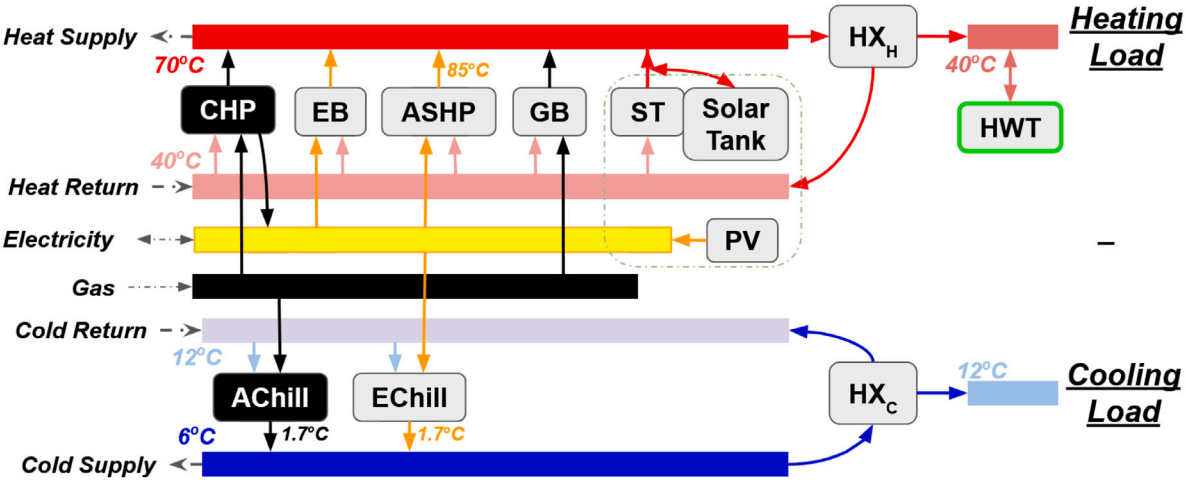

(c) Potential station of a 4G network

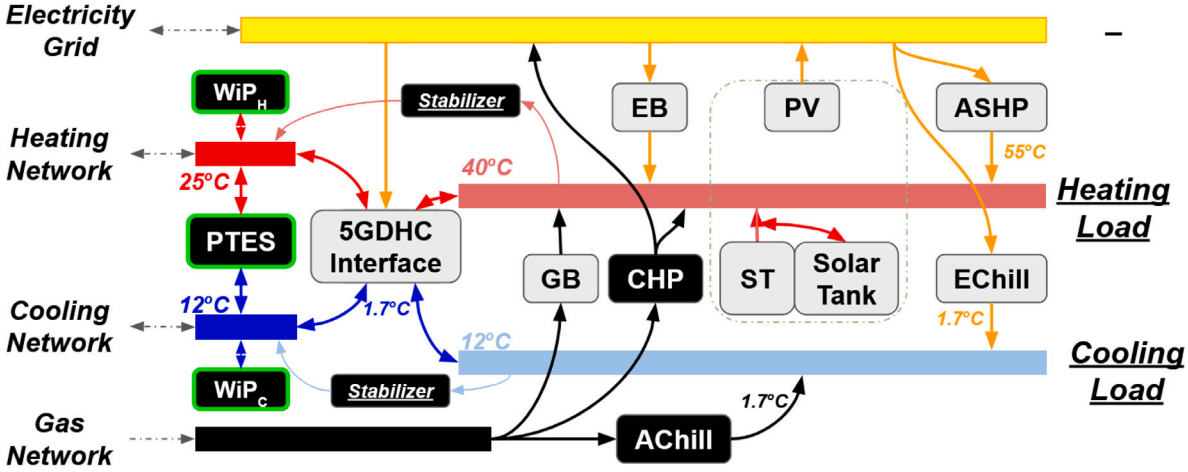

(d) Potential node & station connected to a 5G network

Fig. 3. Potential layouts of nodes.

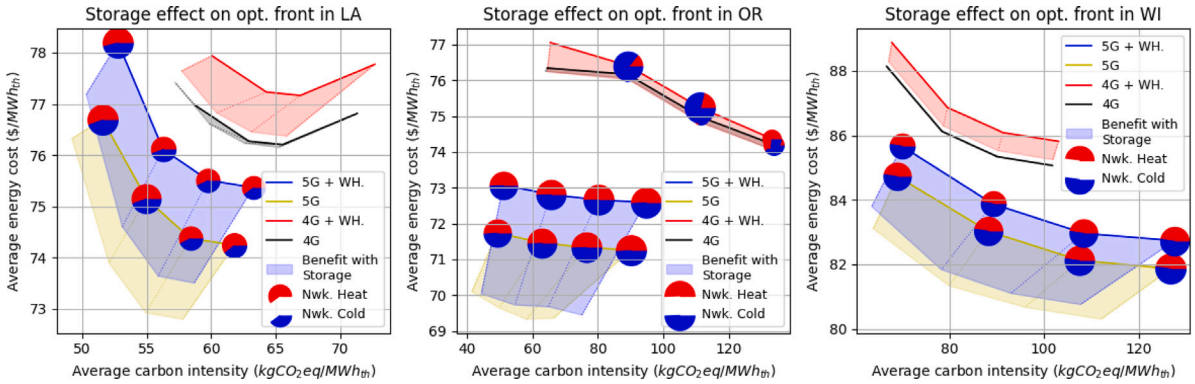

Fig. 4. Pareto fronts of all base scenarios showing the improvements caused by allowing the usage of storage (colored area) and the overall relative connectivity of nodes in the network for each solution (pie charts).

5. Limitations

5.1. Model limitations

We acknowledge the following necessary simplification in the model:

- A MILP formulation is used. It allows simultaneous sizing and operation of all nodes and network. However, it is designed for early stage assessment and is not a "ready to implement" model. The model is based on previously introduced literature. We believe its resolution matches the uncertainty on load and weather at very early design stage.
- Temperature setpoints are set constant prior to computations. No temperature control is included. Consistent temperature levels from related literature [6–9,16,22,32,35,82,83] influenced this choice. These assumptions allow to precompute efficiencies and linearize the model (c.f. Section 3.2). To maintain the scope of the model (e.g. sizing, central-decentral trade-off) and tractability [71], more advanced linearization techniques [42] were not considered.
- Some modeling elements (e.g. non-linear investment costs [71], time varying cost and carbon intensity of electricity) were not included in the study for the sake of simplicity and feasibility of all scenarios.

5.2. Scope limitations

The study breaks down results to gain understandability on how performances are reflected in the energy and investment strategies suggested by the solver. Three cases are selected to offer an overview of similarities and differences over different climates. A systematic in-depth investigation limits the possible number of cases (Section 4.2). However, 3 cases are not sufficient to generalize observations. The impact of different load patterns, heating–cooling overlap (Appendix C), local weather and resource availability is left out of the scope to instead focus on decision mechanisms within the model.

6. Results

An in-depth analysis of base cases is conducted in Section 6.1. Sections 6.2–6.4 extend on the sensitivity of main results to key parameters.

6.1. Base cases: Storage and waste heat

6.1.1. Pareto fronts and connectivity

Results for the base cases are shown in Fig. 4, along with scenarios without storage and WH. The solid lines show cases without storage, the benefit of allowing storage is represented by the colored area. The pie charts show the share of heat and cold delivered by the network, their sizes depict the nodes connectivity.

Pareto fronts for 5G strictly dominate those for 4G in all locations. The 5G DTN is always used, with consistent share and connectivity throughout the decarbonization. The 4G DTN is only used in OR. For this case, an increasing share of cooling transits via the DTN to support decarbonization, except for the most restrictive carbon target. For all other 4G cases, the optimal solution excludes the DTN and focuses on decentralized systems.

The 5G network supplies equivalent shares of heat and cold in all places. This is more beneficial for places with balanced demands. For example, the DTN covers 46% of the heating and 38% of the cooling for a well-balanced demand in OR, but 77% and 14% respectively for the heating and cooling of a cooling dominated demand in LA.

The 4G network benefits from independent heating and cooling sides. When used in OR, it consistently covers 25% of the heating, and 10% to 62% of the cooling. Decentralized HPs are preferred, since high network temperatures limit the efficiency of central HPs. Thus only gas is used to supply heat via the DTN. Central and decentralized chillers have similar efficiencies due to comparable service temperatures, the centralized solution is preferred to reduce investment costs.

The storage increases the financial gap between 4G and 5G cases. Carbon emissions are also reduced, more for 5G cases than 4G. Waste heat always increases costs and emissions. This is compensated by storage in 4G. It is partly shared via the network in OR, which reduces the gap between 4G and 5G there.

The decarbonization cuts up to 75% of what is technically achievable, as loads cannot be reduced. With 5G, the kg of removed carbon emission costs on average ¢42 in LA, ¢1.3 in OR and ¢6.4 in WI. LA can only reduce 14.5% of absolute emissions, while a 41% cut is achieved in OR and WI. For the 4G cases, the transition costs ¢15 in LA, ¢2.7 in OR and ¢8.3 in WI, with respectively 12%, 54% and 34% absolute carbon reduction achieved.

The cost increase is stronger for stricter carbon emission targets. This is particularly visible in LA, where half of the increase happens when going from −50% to −75% emissions. Reasons for this are highlighted in Fig. 5.

6.1.2. Analysis of the energy strategy

Electrification drives the decarbonization for all locations (Fig. 5). It has minor influence on the financial strategy, consisting of 45%–60% of

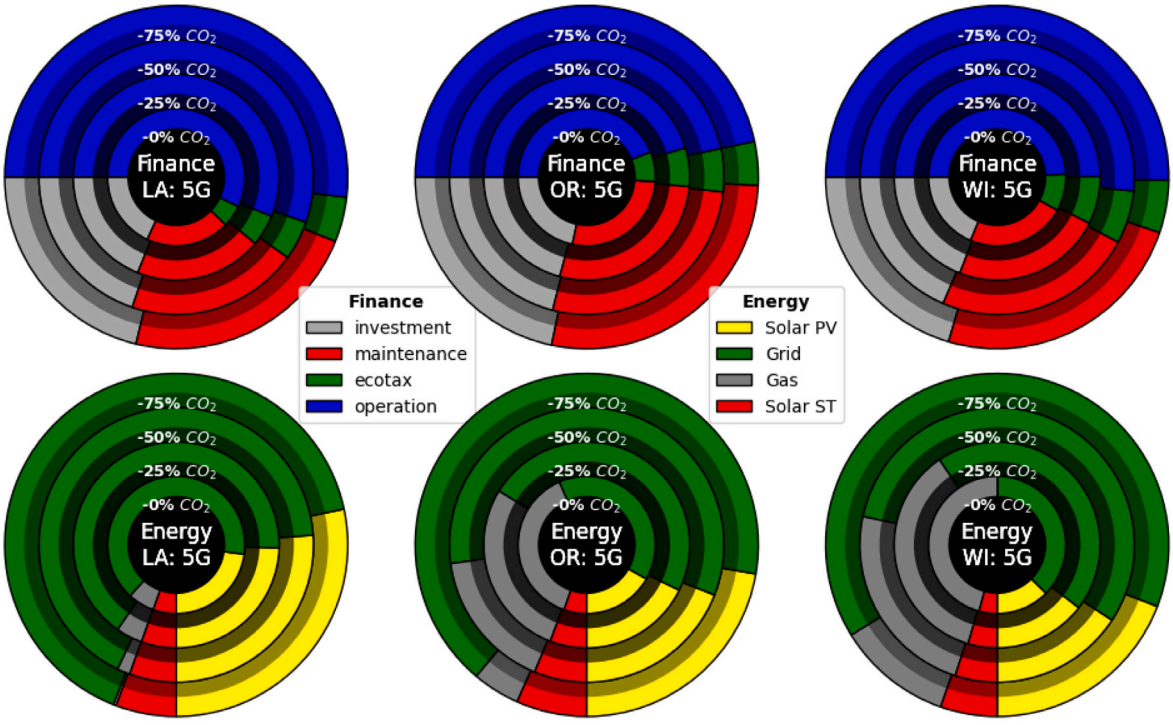

(a) Decarbonization strategies with 5G

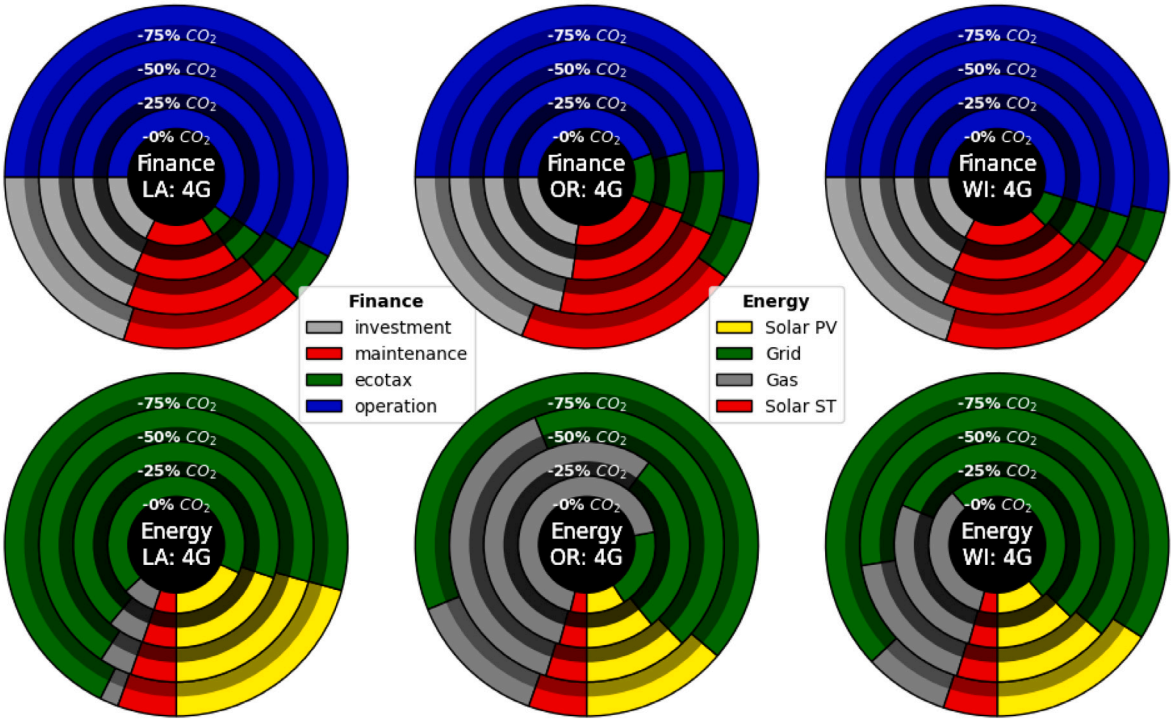

(b) Decarbonization strategies with 4G

Fig. 5. Financial and energy strategies throughout decarbonization, with storage and waste heat included.

operating costs, 35%–45% of maintenance and annualized investment, and 5%–10% of carbon tax. The most significant change is observed for the 4G case in OR: 10% of the cost is transferred from investment and maintenance to operation between −50% and -75% emissions (Fig. 5(b)), i.e. when the 4G network is abandoned (Fig. 4).

The share of gas in the energy mix consistently decreases throughout the decarbonization, replaced by grid and PV electricity. The share of PV electricity is greater in 5G cases than in 4G cases, and this share increases more throughout decarbonization. Inversely, 4G uses more gas and is less able to reduce its usage when decarbonizing.

The energy portfolio differs in every location and explains the different slopes observed in Fig. 4. OR use the most gas at −0%, which is cheap to replace with electricity. LA is almost entirely electrified at −0%. Removing the remaining gas requires costly investments for PV

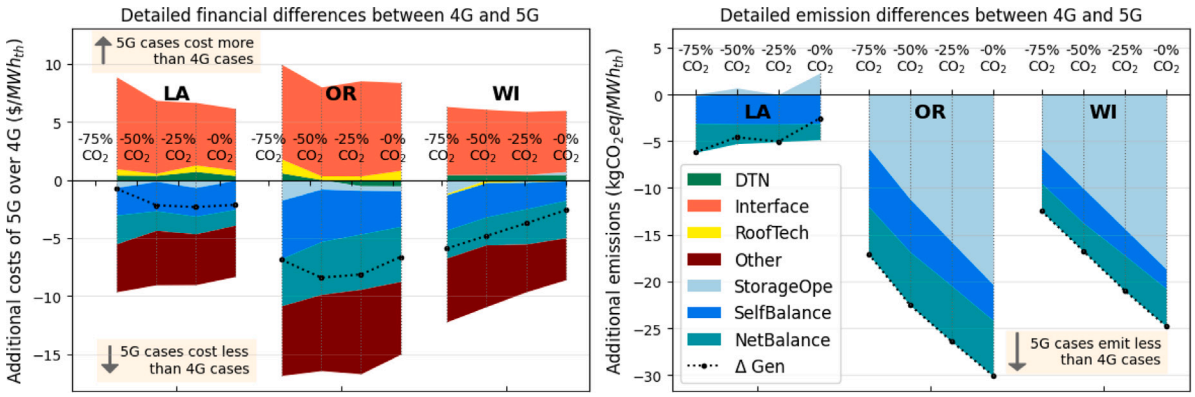

Fig. 6. Detailed difference in costs and emissions between homologous 4G and 5G cases.

and storage for minor reduction of the emissions. WI is an intermediate case where a trade-off of the above occurs.

6.1.3. Difference between 4G and 5G cases

Fig. 6 details the financial (left) and environmental (right) differences between 4G and 5G cases. Positive values mean that 5G cases are more expensive or polluting than their homologous 4G cases in the specified category. The dashed line ΔGen confirms the consistent overall lower cost and carbon intensity of 5G cases.

5G DTN can balance out simultaneous heating and cooling demands within nodes ("SelfBalance") and between nodes ("NetBalance"). This increases the overall system efficiency, with cost decreases of 5G cases over 4G cases valuated from $4\$/MWh_{th}$ in LA to $10\$/MWh_{th}$ in OR. This also consistently reduces emissions by 5–10 $kgCO_2eq/MWh_{th}$.

The interface network-buildings is more expensive and more often used in 5G cases (HP) than 4G cases (HX), representing 5-10$\$/MWh_{th}$ additional costs for 5G cases over 4G cases. However, it is mainly compensated by a reduction in investment for other decentralized generators ("Other"). The remaining investments (roof technologies, storage) weigh little on the financial difference between 4G and 5G, first because both cases benefit from it similarly, second due to the low associated maintenance costs and annualization of the investment. Their impact on the emissions is none as embodied emissions are not considered.

The storage operation ("StorageOpe") brings little financial difference between 4G and 5G cases, but is the main factor explaining differences in emissions in OR and WI. The lower total costs related to storage for 5G cases observed in Fig. 4 are explained by an induced change in the system and in energy strategy, while returned energy itself has minor financial value against fixed grid and gas prices. However, the storage operation cuts carbon emissions up to $20kgCO_2eq/MWh_{th}$ more in 5G cases than in 4G cases. The energy stored and restituted is assumed carbon-free, can be stored in larger quantities in the PTES (5G) than in individual HWT (4G), and can be better redistributed through the 5G DTN. For OR and WI, decarbonization reduces the difference, as 4G cases increase their use of storage. For LA, storage is used little as renewable production is mainly directly used for air-conditioning.

6.2. Financial and environmental parameters

This section presents the sensitivity of results to strategic parameters (c.f. Table 2) for the cases in OR. OR is specifically selected for its representativeness and acceptance of the 4G DTN. Figs. 7–10 have a similar structure and are purposefully dense in information. Sections 6.2.1 to 6.2.4 analyze the overview and major trends from each figure, the reader is free to analyze the figures beyond the textual interpretation.

A block in Figs. 7a to 10a shows the financial difference between two consecutive scenarios for a same network generation for one decarbonization level. The block filling details the contribution of each financial category in the difference. Each block couple covers all three studied scenarios for each case. Block couples of similar decarbonization levels are put side-by-side to facilitate comparison between 4G and 5G. The block frame helps visualizing the network generation. The solid lines show the carbon intensity for each scenario (right axis).

A bar in Figs. 7b to 10b shows the energy strategy of one case under one scenario. The bar filling details the contribution of each energy source in the mix. Each bar triplet covers all three studied scenarios for each case. Bar triplets of similar decarbonization levels are put side-by-side to facilitate comparison between 4G and 5G. The bar frame helps visualizing the network generation. The solid line shows the share of renewable energy in the local production mix (right axis). The size of circles indicates the overall connectivity, i.e. the fraction of thermal energy covered by using the network.

6.2.1. Price of electricity

Both costs and emissions increase with the price of electricity (Fig. 7a), making the decarbonization more expensive. An increasing price of electricity sees grid electricity being replaced by gas and RnE, increasing the operation and investment costs, while making the 4G network more attractive (Fig. 7b). As the increase in electricity price affects the performances of all cases more than a change of DTN technology does, 5G cases remain better than 4G cases in costs, emissions, DTN usage and RnE penetration.

6.2.2. Carbon tax

The carbon tax affects the financial and environmental performances more than a change of DTN technology (Fig. 8a), despite being a minor share of the investment strategy in base cases (Fig. 5). Its increase significantly raises costs at all decarbonization levels, and reduces carbon emissions as much as the enforced decarbonization. When the ecotax goes from 0 to $65\$/t_{CO_2eq}$, its share in the financial strategy explains the cost rise while little changes are observed in the design. From 65$ to 170$, the system design is impacted, and the share of operating and investment costs explains the cost increase. These changes come along with lower energy uses for 4G and 5G cases (Fig. 8b), i.e. an overall increase in efficiency, in which gas is substituted by grid and renewable electricity. Thus the 4GDTN is less attractive while the 5GDTN remains highly used.

6.2.3. Carbon intensity of electricity

A higher carbon intensity of the electricity increases both the costs and carbon emissions. This effect is stronger with stricter carbon targets. Higher carbon intensities limit the decarbonization more in 4G cases than 5G, increasing the gap between them (Fig. 9a). However, the increase in DTN usage is marginal. For -0% and -25% emissions, the

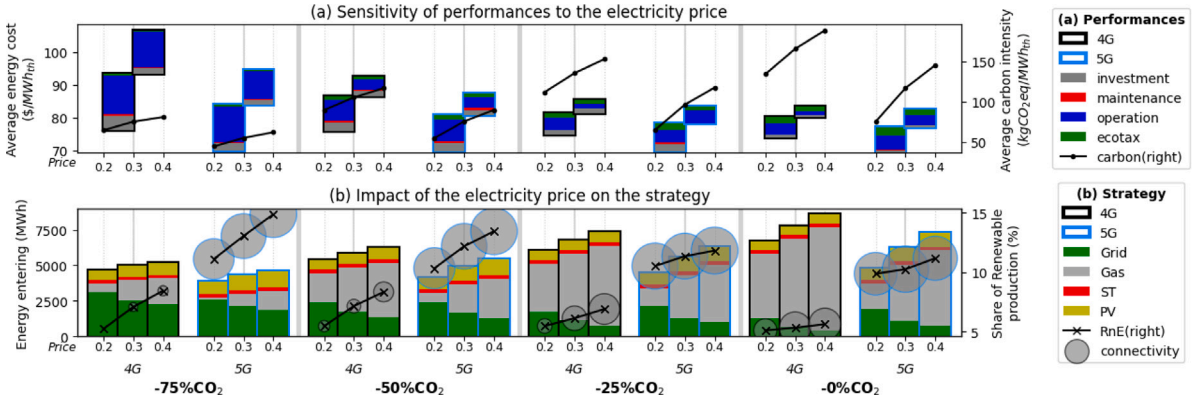

Fig. 7. Effect of the electricity price on 4G and 5G cases in OR.

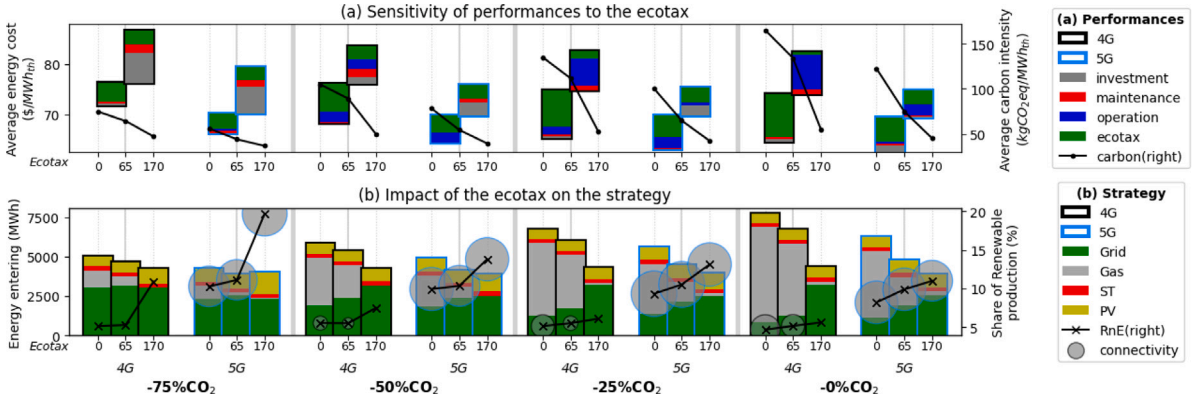

Fig. 8. Effect of the carbon tax on 4G and 5G cases in OR.

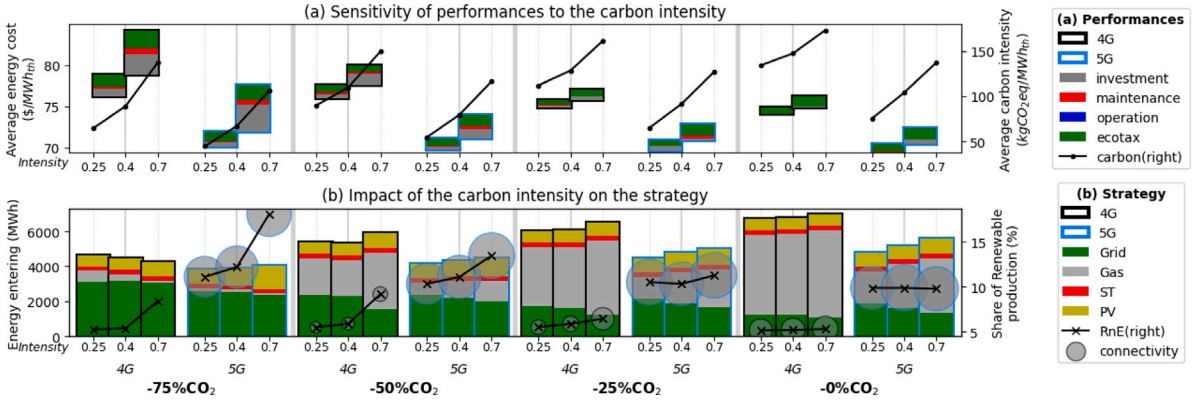

Fig. 9. Effect of the electricity carbon intensity on 4G and 5G cases in OR.

ecotax and higher share of gas cause the mild cost increase (Fig. 9b). For stricter carbon targets, the required cut in gas usage forces system changes, explained by higher shares of RnE and investment costs. The penetration of RnE and its increase are significantly stronger with the 5G case.

6.2.4. Lifetime of equipment

The lifetime relates to the time span over which the annualized investments are spread. Shorter lifetimes have little impact on the overall emissions, while inducing a rise in costs mainly driven by higher investment (Fig. 10a). The gap between 4G and 5G remains unchanged, while the impact of lifetime is greater than these of changing the DTN technology and is consistent throughout decarbonization. The higher investments only reflect the direct link between investment and lifetime, while stable energy strategies reveal that minor structural changes occur in the system (Fig. 10b). Shorter lifetimes slightly reduce the share of gas and RnE, both relying on generation technologies, and the DTN usage is slightly reduced. With these changes the operation costs also contribute to increasing the overall costs.

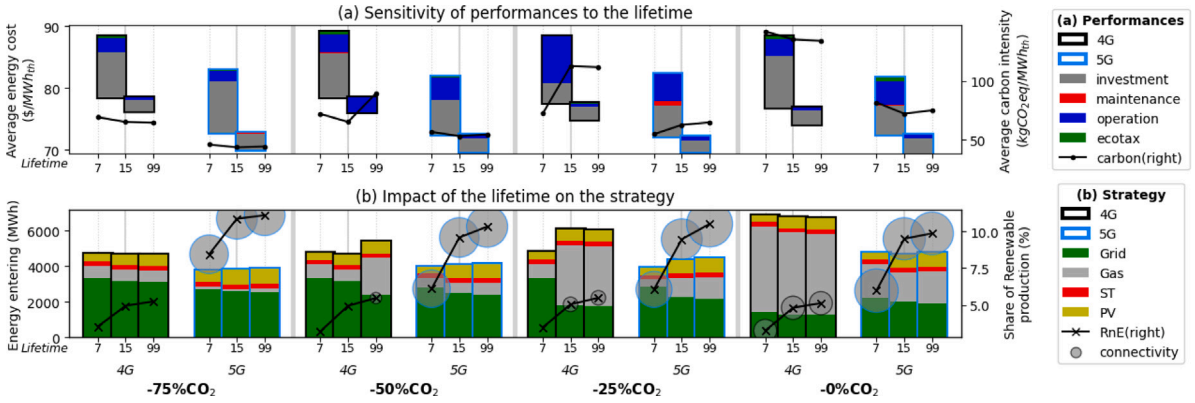

Fig. 10. Effect of the lifetime of assets on 4G and 5G cases in OR.

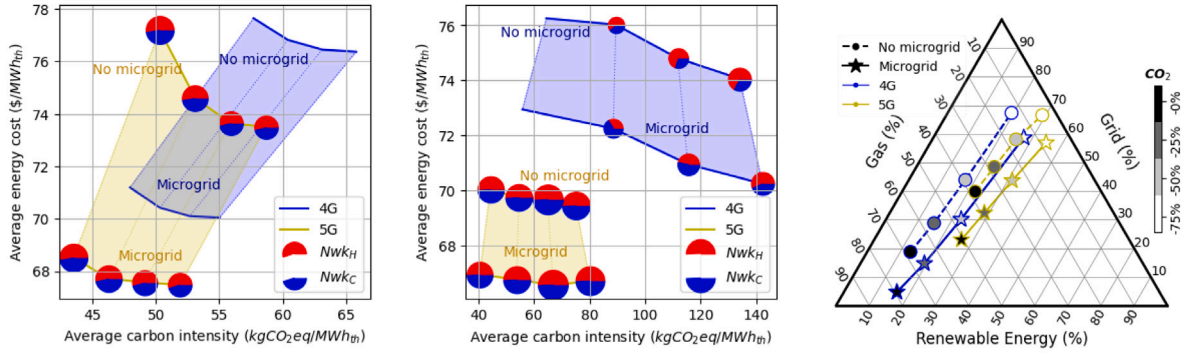

(a) Financial impact in LA (b) Financial impact in OR (c) Impact on the energy mix in OR

Fig. 11. Impact of accounting for local electricity at the district level.

6.3. Micro-grid

A micro-grid model was added to allow an electrical connection between buildings. The micro-grid simply considers DC lines and the cost of infrastructure is not considered. This is suggested to study the impact of accounting for locally generated electricity. Indeed, buildings generate PV electricity and feed surplus back into the grid. However, that electricity is likely to flow directly to a neighbor building in need.

Figs. 11(a) and 11(c) show the effect on financial and environmental performances of accounting for local renewable generation. A drop in costs is observed with local electricity. This decrease is twice as important as the financial gap between 4G and 5G in LA, while being equivalent to the gap in WA and half of it in OR. Additional cooling is supplied via the 4G DTN in OR, while the 4G DTN remains unused in other locations. The usage of 5G DTN remains unchanged. Accounting for local electricity reduces carbon emissions in LA and WI, where cooling and RnE potential align, however hardly impacts decarbonizing in OR.

The consequences on the energy strategy are shown in Fig. 11(c) for OR, with similar trends in other locations. The share of gas increases with local electricity. This effect is stronger in OR, explaining the lack of carbon benefits there. With local electricity, the share of RnE systematically increases by 10%, and rises 10% more over the decarbonization instead of 7%. The rest of the strategy behind decarbonization is unchanged, with grid electricity replacing gas.

6.4. Topology and energy station

Different scenarios were tested for the topology and building hosting the main energy station.

Fig. 12 shows the best and worst performing combination of topology and building type hosting the central energy station. With a favorable topology and station location, the usage of a 4G DTN can become viable (Fig. 12(a)) and improve performances of 4G cases (Fig. 12(b)). Performances of 5G cases can also be impacted, and the 5G DTN usage may be less consistent. A different topology and station location may result in close comparisons between 5G and standalone (Fig. 12(c)), 5G and 4G DTN (Fig. 12(b)) or even make 4G DTN more financially attractive than 5G (Fig. 12(a)).

7. Discussion

The heat-cold balancing within a building allowed with 5G networks represents a significant advantage in this study. This is technically allowed by the usage of independent HP and EChill interacting with the network [9]. This effect could be reduced or canceled with buildings having no concurrent loads or using VRF and advanced HVAC systems. However, 4G networks only focus on delivering thermal energy at the supply temperature required by buildings and need the required temperature to be homogeneous across the network. 5G networks are rather associated with high quality buildings, thus the data and network interaction as implemented, seem reasonable.

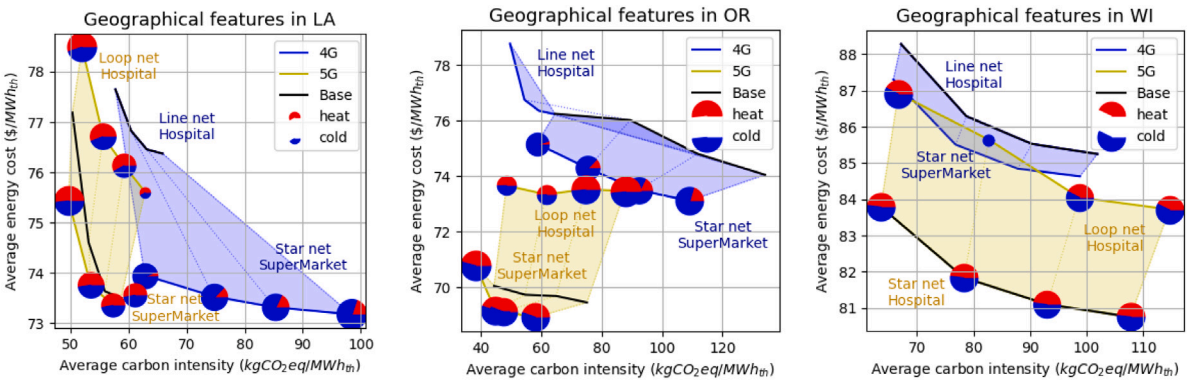

(a) Performances in LA (b) Performances in OR (c) Performances in WI

Fig. 12. Performances of different topologies and building types hosting the main energy station.

The share of energy via the network represents another major part of the superiority of 5G networks over 4G networks, while most related literature concludes on the superiority of centralized systems. The current network model is based on energy transfer, as implemented by Wirtz et al. [9,71,77,84] and used in estimates of 5G network potential [47,83,85,86]. It also aligns with 4G models commonly used in literature [32,35–37]. More generally, this energy transfer paradigm using MILP was found accurate when confronted to real data [40] for a 5G network, and even verified against simulation for a 4G case [36]. It differs from temperature-based networks in comparative studies using optimization and simulation [8,16–22], which is supposed to be more accurate. For example, Gross et al. [18] verified the fluid-dynamic aspect of their simulation approach against real data.

An additional explanation may be found in the case study and share of cooling in the demand. Table 1 shows that most authors comparing both technologies do so with little load diversity, and when the diversity exists, chosen cases show a largely dominating heating demand. The study by Zhang et al. [86] shows conditions and types of buildings most suited to boost efficiency of a 5G network. It happens to match with the combinations of building types and climates we chose.

The observations are only valid within the reduced pool of cases. Other conditions (weather, resource availability, load patterns, concurrent heat and cooling demands, number of buildings, load density, temperature set points and controls) influence the performances of DTN based MES. Their importance needs further quantification through a significantly larger pool of cases.

Specifically, temperature integration and control have significant impacts on DTN flexibility and efficiency. This study focuses on early stage design assessment, temperature approximations are assumed to level the high uncertainty of loads and weather conditions. Later and more informed stages of development would benefit from additional information (e.g. varying prices and carbon intensity of electricity) and control (e.g. temperature control) to better implement informed control strategy.

Including more information at early stage design is appealing but faces limitations. Limitations may reside in the need of drastic simplifications on other model aspects. Or burdensome iterative processes relying on advanced tools must be used [87]. For the latter, future work is needed to build fast and reliable surrogate models to replace burdensome advanced tools in such iterative process.

The current study also highlights the need for further investigation about 5G network modeling. The ability to balance energy is at the center of interest for 5G networks, however its implementation and results in the current study may be controversial. Future work should focus on assessing the importance and technicity of the energy sharing through a 5G network.

8. Conclusion

The selection network technology in the development of energy projects must be addressed at early-stage design. The present study implements a linear energy hub model encompassing specific characteristics of both 4th (4G) and 5th generation (5G) district heating and cooling networks, including the strong warm/cold coupling of 5G technologies. The model is challenged across a variety of scenarios for districts with a mix of building types.

The 5G is found to perform financially and environmentally better than 4G. This differs with results from related literature. The ability to balance out simultaneous heating and cooling demands across the 5G network explains most of the difference. It overtakes the higher investment for decentralized heat pumps. The current energy-based model uses a different paradigm than most literature comparing 4G and 5G, which is based on network temperature. Both paradigms were validated in publications and against simulation and real data. However, the latter does not seem to capture this balancing ability across the 5G network.

Results should be further nuanced due to the model sensitivity in critical parameters. Annualized models amplify the role of operation and minimize these of investments, which strongly differs from common practice accounting for shorter ROI periods. Moreover, potential topology and the spacial spread of loads within the network is found to significantly impact the difference between the two network technologies, possibly making 4G more profitable than 5G in specific climate zones.

The difference between the temperature and energy paradigms in the modeling of 5G networks requires further investigation. The computationally intensive requirements of such models does not allow statistically rigorous sensitivity analysis and limits the integration of temperature control, which motives further development in surrogate modeling for district thermal network.

Acknowledgments

This research is supported by the NSERC Alliance Grant ALLRP 566285 via the ReBuild initiative (https://rebuild.uvic.ca/).

CRediT authorship contribution statement

François Lédée: Writing – review & editing, Writing – original draft, Visualization, Validation, Software, Project administration, Methodology, Investigation, Formal analysis, Data curation, Conceptualization. **Ralph Evins:** Supervision, Funding acquisition.

Declaration of competing interest

The authors declare that they have no known competing financial interests or personal relationships that could have appeared to influence the work reported in this paper.

Appendix A. Parameters

The prices and parameters of the model are issued from commercial data, vendor websites, and related publications (see Tables A.1–A.3). Details about the price calculations can be found in the repository.[5]

Costs, schedules ϵ and thermal capacities λ differ between 4G and 5G links due to the absence of insulation for the latter. Costs differ between Supply/Return and Warm/Cold due to groundwork estimated as 285 $/m [9] and accounted for only once. Thus, we assume cold and warm 4G networks require separate groundwork.

The efficiencies "pre" are precomputed efficiencies for every time step t (see Section 4). The specific investment cost of ST results from a combination of factors: positive fixed costs, subsidies in most cases used to evaluate the cost, a minimum installation capacity to ensure a positive investment cost (see document available in the repository) A proportionality coefficient of 5.7 is enforced between the installed capacities of ST and Solar Tank.

Table A.1
Technico-financial parameters for the network pipes.

	C^{fix} ($/m)	C^{lin} ($/kW m)	Δp_x (Pa/m)	D (mm)	ϵ (mm)	λ (W/m K)	life (y)	L (m)
Supply 4G	387	0.03	200	250	44	0.04	30	200
Return 4G	102	0.03	200	250	44	0.04	30	200
Warm 5G	385	0.03	200	250	20	0.4	30	200
Cold 5G	100	0.03	200	250	20	0.4	30	200

Table A.2
Parameters of converters.

	C^{fix} ($)	C^{lin} ($/kW)	$C^{O\&M}$ ($/kW)	$H_{\sigma,\tau}$	life (y)
PV	0	1020	9.7	pre	20
ST	−1366	1213	18.3	pre	25
GB	1492	47	15.6	0.925	25
EB	95	219	7.31	0.98	25
AChill	2460	664	11.6	0.72	20
CHP	3000	1150	42.5	0.37/0.46	20
ASHP	2968	198	32.5	pre	20
EChill	2968	198	32.5	pre	20
5G Interface	3876	115	83.2	pre	25
4G HX	0	100	1.1	1	20
Central GB	1268	40	13.3	0.98	25
Central EB	81	186	6.2	1	25
Central ASHP	2523	168	27.6	pre	20
Central EChill	2523	168	27.6	pre	20

[5] https://gitlab.com/fledee/detail_network

Table A.3
Parameters for storage.

	Solar Tank	HWT	WiP	PTES
C^{fix} ($)	0*	225	0**	554
C^{lin} ($/kWh)	0*	79	0**	0.4
$C^{o\&m}$ ($/kWh)	–	–	–	–
β^{ch}/β^{dch}	0.3	0.5	0.2	**
κ	0.05	0.05	0.038	0.001
η^{ch}/η^{dch}	1	1	1	1
life (y)	20	20	30	30

* Costs in ST, capacity is 5.7 × ST.
** Related to network links.

Appendix B. 5G interface

The unit is composed of three elements: a water sourced HP, a water sourced chiller and a balancing unit (see Fig. B.1). The HP and chiller consume electricity to pump water in one pipe, process it and reject the downgraded water in the other network pipe. The amount of thermal energy retrieved, fed back and transferred to the building equal the electricity input divided by the efficiency ($\dot{Q}_t^{el}/COP_t$). This principle represents the operation of 5G DTNs. For the building to also feed energy, the *balance* element is needed. It can cancel out 1 unit of active heat with one of active cold. Feeding an extra unit of heat to the network is equivalent to cooling the building down: (1) importing cold from the network, which generates the heat in the network, then (2) cancel out this imported cold with the excess heat.

This does not affect the heating and cooling demands, which must still be met. However, a simultaneous usage of the HP and chiller allows to cover simultaneous heating and cooling demands, exploiting the network locally with no generation of thermal energy, and at the only expense of the electricity bill to use both devices simultaneously.

Appendix C. Building data overlap

The total thermal load of every node type was described in Table 4 of Section 4. The potential of 5G networks also relies on the simultaneous heating and cooling demands [9]. As a way to measure it, the Demand Overlap Coefficient (DOC) was suggested by Wirtz et al. [83]. The DOC Φ is expressed in Eq. (25), where $\dot{Q}_{n,H,t}^{Load}$ and $\dot{Q}_{n,C,t}^{Load}$ are the heating and cooling loads at every time step t. Its value lies between 0% and 100%, with 100% meaning both loads are identical.

$$\Phi = \frac{2 \cdot \sum_{t\in\mathbb{T}} \min\{\dot{Q}_{n,H,t}^{Load}, \dot{Q}_{n,C,t}^{Load}\}}{\sum_{t\in\mathbb{T}}(\dot{Q}_{n,H,t}^{Load} + \dot{Q}_{n,C,t}^{Load})} \tag{25}$$

The DOC Φ was calculated for every possible combination of node type considered in this study (Hospital, Apartments, SuperMarket, Offices). Fig. C.1 displays the DOC values, detailed by number of combined nodes. Hospital and Apartments have the highest DOC for single nodes. Highest DOCs in all locations arise from combinations of two or three node types among Hospital, Apartments and SuperMarket. Fig. C.1 also shows the DOC is overall lower in LA, at best 40%, and higher in OR, with values up to 70%.

Data availability

A git repository containing the data, codes and estimates of financial parameters is made available at https://gitlab.com/fledee/detail_network.

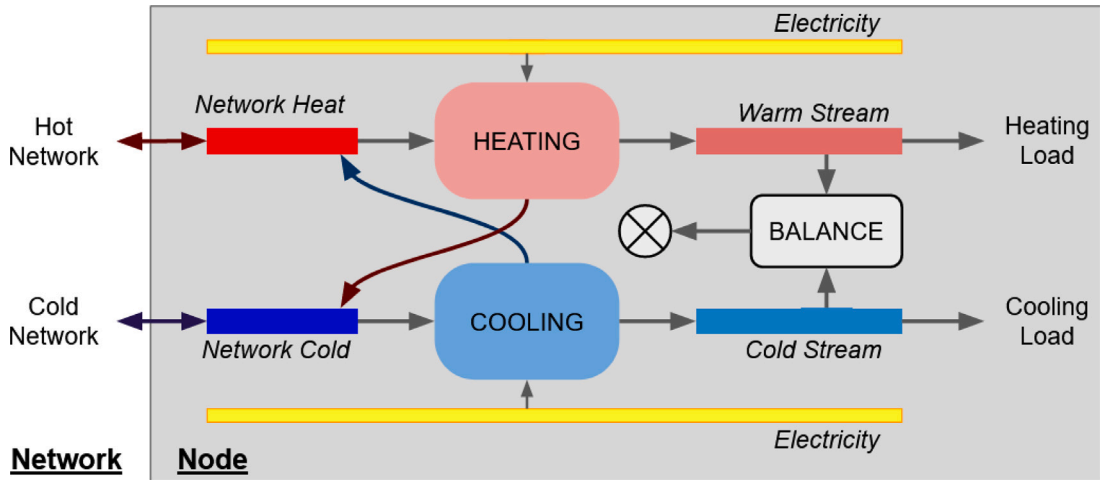

Fig. B.1. Detailed principle of the interaction 5G DTN - Node.

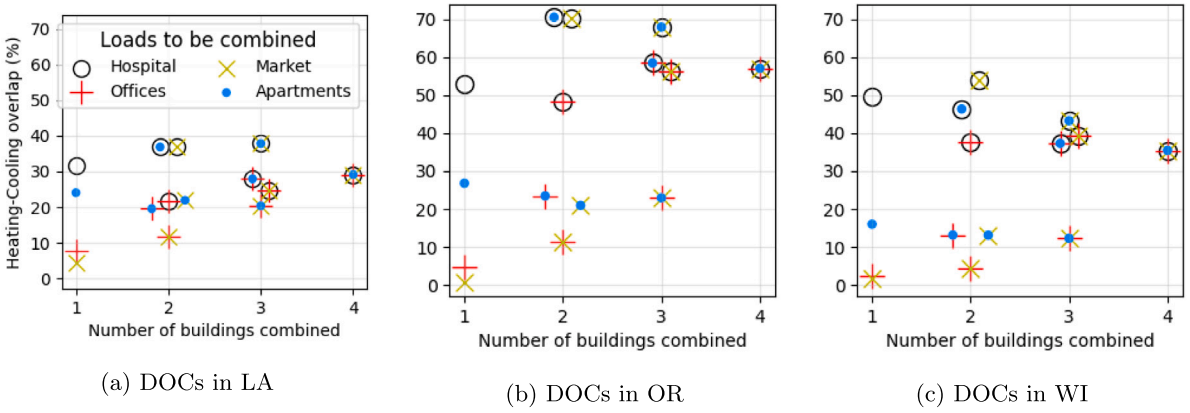

Fig. C.1. Ratio of simultaneous heating and cooling for all possible combinations of loads.

References

[1] Mavromatidis G, Orehounig K, Bollinger LA, Hohmann M, Marquant JF, Miglani S, et al. Ten questions concerning modeling of distributed multi-energy systems. Build Environ 2019;165:106372. http://dx.doi.org/10.1016/j.buildenv.2019.106372.

[2] Aunedi M, Pantaleo AM, Kuriyan K, Strbac G, Shah N. Modelling of national and local interactions between heat and electricity networks in low-carbon energy systems. Appl Energy 2020;276:115522. http://dx.doi.org/10.1016/j.apenergy.2020.115522.

[3] Gjoka K, Rismanchi B, Crawford RH. Fifth-generation district heating and cooling systems: A review of recent advancements and implementation barriers. Renew Sustain Energy Rev 2023;171:112997. http://dx.doi.org/10.1016/j.rser.2022.112997.

[4] Fabozzi S, De Luca G, Vanoli L. Chapter 9 - fourth generation district heating and cooling. In: Calise F, D'Accadia M Dentice, Vanoli L, Vicidomini M, editors. Polygeneration systems. Academic Press; 2022, p. 323–50. http://dx.doi.org/10.1016/B978-0-12-820625-6.00003-7.

[5] Buffa S, Cozzini M, D'Antoni M, Baratieri M, Fedrizzi R. 5Th generation district heating and cooling systems: A review of existing cases in Europe. Renew Sustain Energy Rev 2019;104:504–22. http://dx.doi.org/10.1016/j.rser.2018.12.059.

[6] Lund H, Østergaard PA, Nielsen TB, Werner S, Thorsen JE, Gudmundsson O, et al. Perspectives on fourth and fifth generation district heating. Energy 2021;227:120520. http://dx.doi.org/10.1016/j.energy.2021.120520.

[7] Østergaard PA, Werner S, Dyrelund A, Lund H, Arabkoohsar A, Sorknæs P, et al. The four generations of district cooling - A categorization of the development in district cooling from origin to future prospect. Energy 2022;253:124098. http://dx.doi.org/10.1016/j.energy.2022.124098.

[8] Nérot B, Lamaison N, Mabrouk M, Bavière R, Lacarrière B. Optimization framework for evaluating urban thermal systems potential. Energy 2023;270:126851. http://dx.doi.org/10.1016/j.energy.2023.126851.

[9] Wirtz M, Kivilip L, Remmen P, Müller D. 5Th generation district heating: A novel design approach based on mathematical optimization. Appl Energy 2020;260:114158. http://dx.doi.org/10.1016/j.apenergy.2019.114158.

[10] Bilardo M, Sandrone F, Zanzottera G, Fabrizio E. Modelling a fifth-generation bidirectional low temperature district heating and cooling (5GDHC) network for nearly zero energy district (nZED). Energy Rep 2021;7:8390–405. http://dx.doi.org/10.1016/j.egyr.2021.04.054.

[11] Geidl M, Koeppel G, Favre-Perrod P, Klöckl B, Andersson G, Fröhlich K. The energy hub-A powerful concept for future energy systems. In: Third annual carnegie mellon conference on the electricity industry. Pittsburg: Carnegie Mellon; 2007, p. 13–4.

[12] Lindhe J, Javed S, Johansson D, Bagge H. A review of the current status and development of 5GDHC and characterization of a novel shared energy system. Sci Technol Built Environ 2022;28(5):595–609. http://dx.doi.org/10.1080/23744731.2022.2057111.

[13] Mohammadi M, Noorollahi Y, Mohammadi-Ivatloo B, Yousefi H. Energy hub: From a model to a concept – A review. Renew Sustain Energy Rev 2017;80:1512–27. http://dx.doi.org/10.1016/j.rser.2017.07.030.

[14] Evins R, Orehounig K, Dorer V, Carmeliet J. New formulations of the 'energy hub' model to address operational constraints. Energy 2014;73:387–98. http://dx.doi.org/10.1016/j.energy.2014.06.029.

[15] Terlouw T, Gabrielli P, AlSkaif T, Bauer C, McKenna R, Mazzotti M. Optimal economic and environmental design of multi-energy systems. Appl Energy 2023;347:121374. http://dx.doi.org/10.1016/j.apenergy.2023.121374.

[16] Brumana G, Franchini G, Ghirardi E, Ravelli S. Optimization of solar district heating & cooling systems. J Phys Conf Ser 2022;2385(1):012113. http://dx.doi.org/10.1088/1742-6596/2385/1/012113.

[17] Calise F, Cappiello FL, Cimmino L, d'Accadia MD, Vicidomini M. A comparative thermoeconomic analysis of fourth generation and fifth generation district heating and cooling networks. Energy 2023;128561. http://dx.doi.org/10.1016/j.energy.2023.128561.

[18] Gross M, Karbasi B, Reiners T, Altieri L, Wagner H-J, Bertsch V. Implementing prosumers into heating networks. Energy 2021;230:120844. http://dx.doi.org/10.1016/j.energy.2021.120844.

[19] Gudmundsson O, Schmidt R-R, Dyrelund A, Thorsen JE. Economic comparison of 4GDH and 5GDH systems – Using a case study. Energy 2022;238:121613. http://dx.doi.org/10.1016/j.energy.2021.121613.

[20] Jebamalai JM, Marlein K, Laverge J. Design and cost comparison of district heating and cooling (DHC) network configurations using ring topology – A case study. Energy 2022;258:124777. http://dx.doi.org/10.1016/j.energy.2022.124777.
[21] Zhang Y, Johansson P, Sasic Kalagasidis A. Assessment of district heating and cooling systems transition with respect to future changes in demand profiles and renewable energy supplies. Energy Convers Manage 2022;268:116038. http://dx.doi.org/10.1016/j.enconman.2022.116038.
[22] Millar M-A, Yu Z, Burnside N, Jones G, Elrick B. Identification of key performance indicators and complimentary load profiles for 5th generation district energy networks. Appl Energy 2021;291:116672. http://dx.doi.org/10.1016/j.apenergy.2021.116672.
[23] Bordin C, Gordini A, Vigo D. An optimization approach for district heating strategic network design. European J Oper Res 2016;252(1):296–307. http://dx.doi.org/10.1016/j.ejor.2015.12.049.
[24] Résimont T, Louveaux Q, Dewallef P. Optimization tool for the strategic outline and sizing of district heating networks using a geographic information system. Energies 2021;14(17):5575. http://dx.doi.org/10.3390/en14175575, number: 17 Publisher: Multidisciplinary Digital Publishing Institute.
[25] Chen D, Abbas Z, Li Y, Hu X, Zeng S, Liu Y. Optimal centralized integrated energy station site approach based on energy transmission loss analysis. Int J Energy Res 2021;45(1):894–907. http://dx.doi.org/10.1002/er.5980.
[26] Kuriyan K, Shah N. A combined spatial and technological model for the planning of district energy systems. Int. J. Sustain. Energy Plan. Manage. 2019;21. http://dx.doi.org/10.5278/IJSEPM.2019.21.8, (2019)Publisher: International Journal of Sustainable Energy Planning and Management.
[27] Lorestani A, Chebeir J, Narimani M, Cotton JS. Multi-objective optimization of integrated community energy and harvesting (ICE-Harvest) system based on marginal emission factor. In: 2021 IEEE international smart cities conference. 2021, p. 1–7. http://dx.doi.org/10.1109/ISC253183.2021.9562882.
[28] Fiorentini M, Heer P, Baldini L. Design optimization of a district heating and cooling system with a borehole seasonal thermal energy storage. Energy 2023;262:125464. http://dx.doi.org/10.1016/j.energy.2022.125464.
[29] Petkov I, Gabrielli P. Power-to-hydrogen as seasonal energy storage: an uncertainty analysis for optimal design of low-carbon multi-energy systems. Appl Energy 2020;274:115197. http://dx.doi.org/10.1016/j.apenergy.2020.115197.
[30] Petkov I, Gabrielli P, Spokaite M. The impact of urban district composition on storage technology reliance: Trade-offs between thermal storage, batteries, and power-to-hydrogen. Energy 2021;224:120102. http://dx.doi.org/10.1016/j.energy.2021.120102.
[31] Murray P, Orehounig K, Grosspietsch D, Carmeliet J. A comparison of storage systems in neighbourhood decentralized energy system applications from 2015 to 2050. Appl Energy 2018;231:1285–306. http://dx.doi.org/10.1016/j.apenergy.2018.08.106.
[32] Morvaj B, Evins R, Carmeliet J. Decarbonizing the electricity grid: The impact on urban energy systems, distribution grids and district heating potential. Appl Energy 2017;191:125–40. http://dx.doi.org/10.1016/j.apenergy.2017.01.058.
[33] Dorotić H, Pukšec T, Duić N. Multi-objective optimization of district heating and cooling systems for a one-year time horizon. Energy 2019;169:319–28. http://dx.doi.org/10.1016/j.energy.2018.11.149.
[34] Unternährer J, Moret S, Joost S, Maréchal F. Spatial clustering for district heating integration in urban energy systems: Application to geothermal energy. Appl Energy 2017;190:749–63. http://dx.doi.org/10.1016/j.apenergy.2016.12.136.
[35] Morvaj B, Evins R, Carmeliet J. Optimising urban energy systems: Simultaneous system sizing, operation and district heating network layout. Energy 2016;116:619–36. http://dx.doi.org/10.1016/j.energy.2016.09.139.
[36] Wang D, Li X, Marquant J, Carmeliet J, Orehounig K. Advancing the thermal network representation for the optimal design of distributed multi-energy systems. Front Energy Res 2021;9:668124. http://dx.doi.org/10.3389/fenrg.2021.668124.
[37] Marquant JF, Evins R, Bollinger LA, Carmeliet J. A holarchic approach for multi-scale distributed energy system optimisation. Appl Energy 2017;208:935–53. http://dx.doi.org/10.1016/j.apenergy.2017.09.057.
[38] Pantaleo AM, Giarola S, Bauen A, Shah N. Integration of biomass into urban energy systems for heat and power. Part II: Sensitivity assessment of main techno-economic factors. Energy Convers Manage 2014;83:362–76. http://dx.doi.org/10.1016/j.enconman.2014.03.051.
[39] Pantaleo AM, Giarola S, Bauen A, Shah N. Integration of biomass into urban energy systems for heat and power. Part I: An MILP based spatial optimization methodology. Energy Convers Manage 2014;83:347–61. http://dx.doi.org/10.1016/j.enconman.2014.03.050.
[40] Prasanna A, Dorer V, Vetterli N. Optimisation of a district energy system with a low temperature network. Energy 2017;137:632–48. http://dx.doi.org/10.1016/j.energy.2017.03.137.
[41] Wirtz M, Neumaier L, Remmen P, Müller D. Temperature control in 5th generation district heating and cooling networks: An MILP-based operation optimization. Appl Energy 2021;288:116608. http://dx.doi.org/10.1016/j.apenergy.2021.116608.
[42] Gabrielli P, Acquilino A, Siri S, Bracco S, Sansavini G, Mazzotti M. Optimization of low-carbon multi-energy systems with seasonal geothermal energy storage: The anergy grid of ETH zurich. Energy Convers Manage X 2020;8:100052. http://dx.doi.org/10.1016/j.ecmx.2020.100052.
[43] Taylor M, Long S, Marjanovic O, Parisio A. Model predictive control of smart districts with fifth generation heating and cooling networks. IEEE Trans Energy Convers 2021;36(4):2659–69. http://dx.doi.org/10.1109/TEC.2021.3082405, conference Name: IEEE Transactions on Energy Conversion.
[44] Brown A, Foley A, Laverty D, McLoone S, Keatley P. Heating and cooling networks: A comprehensive review of modelling approaches to map future directions. Energy 2022;261:125060. http://dx.doi.org/10.1016/j.energy.2022.125060.
[45] Lyden A, Brown C, Kolo I, Falcone G, Friedrich D. Seasonal thermal energy storage in smart energy systems: District-level applications and modelling approaches. Renew Sustain Energy Rev 2022;167:112760. http://dx.doi.org/10.1016/j.rser.2022.112760.
[46] von Rhein J, Henze GP, Long N, Fu Y. Development of a topology analysis tool for fifth-generation district heating and cooling networks. Energy Convers Manage 2019;196:705–16. http://dx.doi.org/10.1016/j.enconman.2019.05.066.
[47] Abugabbara M, Javed S, Johansson D. A simulation model for the design and analysis of district systems with simultaneous heating and cooling demands. Energy 2022;261:125245. http://dx.doi.org/10.1016/j.energy.2022.125245.
[48] Quirosa G, Torres M, Chacartegui R. Analysis of the integration of photovoltaic excess into a 5th generation district heating and cooling system for network energy storage. Energy 2022;239:122202. http://dx.doi.org/10.1016/j.energy.2021.122202.
[49] Saini P, Huang P, Fiedler F, Volkova A, Zhang X. Techno-economic analysis of a 5th generation district heating system using thermo-hydraulic model: A multi-objective analysis for a case study in heating dominated climate. Energy Build 2023;296:113347. http://dx.doi.org/10.1016/j.enbuild.2023.113347.
[50] Maccarini A, Sotnikov A, Sommer T, Wetter M, Sulzer M, Afshari A. Influence of building heat distribution temperatures on the energy performance and sizing of 5th generation district heating and cooling networks. Energy 2023;275:127457. http://dx.doi.org/10.1016/j.energy.2023.127457.
[51] Bu T, Fan R, Zheng B, Sun K, Zhou Y. Design and operation investigation for the fifth-generation heating and cooling system based on load forecasting in business districts. Energy Build 2023;294:113243. http://dx.doi.org/10.1016/j.enbuild.2023.113243.
[52] Calise F, Cappiello FL, Dentice d'Accadia M, Petrakopoulou F, Vicidomini M. A solar-driven 5th generation district heating and cooling network with ground-source heat pumps: A thermo-economic analysis. Sustainable Cities Soc 2022;76:103438. http://dx.doi.org/10.1016/j.scs.2021.103438.
[53] Youn YJ, Im YH. Analysis of operating characteristics of interconnected operation of thermal grids with bidirectional heat trade. Appl Therm Eng 2023;229:120608. http://dx.doi.org/10.1016/j.applthermaleng.2023.120608.
[54] Taylor M, Gao W, Masum S, Qadrdan M. Techno-economic assessment of bi-directional low temperature networks. Appl Energy 2023;347:121202. http://dx.doi.org/10.1016/j.apenergy.2023.121202.
[55] Belliardi M, Caputo P, Ferla G, Cereghetti N, Antonioli Mantegazzini B. An innovative application of 5GDHC: A techno-economic assessment of shallow geothermal systems potential in different European climates. Energy 2023;280:128104. http://dx.doi.org/10.1016/j.energy.2023.128104.
[56] Hirsch H, Nicolai A. An efficient numerical solution method for detailed modelling of large 5th generation district heating and cooling networks. Energy 2022;255:124485. http://dx.doi.org/10.1016/j.energy.2022.124485.
[57] Allen A, Henze G, Baker K, Pavlak G, Murphy M. An optimization framework for the network design of advanced district thermal energy systems. Energy Convers Manage 2022;266:115839. http://dx.doi.org/10.1016/j.enconman.2022.115839.
[58] Qin Q, Gosselin L. Multiobjective optimization and analysis of low-temperature district heating systems coupled with distributed heat pumps. Appl Therm Eng 2023;230:120818. http://dx.doi.org/10.1016/j.applthermaleng.2023.120818.
[59] Best I. Economic comparison of low-temperature and ultra-low-temperature district heating for new building developments with low heat demand densities in Germany. Int J Sustain Energy Plan Manage 2018;45–60. http://dx.doi.org/10.5278/IJSEPM.2018.16.4, PáginasArtwork Size: 45-60 Páginas Publisher: International Journal of Sustainable Energy Planning and Management.
[60] Best I, Orozaliev J, Vajen K. Impact of different design guidelines on the total distribution costs of 4th generation district heating networks. Energy Procedia 2018;149:151–60. http://dx.doi.org/10.1016/j.egypro.2018.08.179.
[61] Sorknæs P, Østergaard PA, Thellufsen JZ, Lund H, Nielsen S, Djørup S, Sperling K. The benefits of 4th generation district heating in a 100% renewable energy system. Energy 2020;213:119030. http://dx.doi.org/10.1016/j.energy.2020.119030.
[62] Gurobi. Mixed-Integer Programming (MIP) - A Primer on the Basics. https://www.gurobi.com/resource/mip-basics/.
[63] Murray P, Carmeliet J, Orehounig K. Multi-objective optimisation of power-to-mobility in decentralised multi-energy systems. Energy 2020;205:117792. http://dx.doi.org/10.1016/j.energy.2020.117792.
[64] Arnfalk O. Modeling energy losses and gains in low temperature bi-directional heating and cooling grids [Thesis], M.Sc and Engineering, Lund University, Lund; 2022.
[65] Song Y, Yao Y, Na W. Impacts of soil and pipe thermal conductivity on performance of horizontal pipe in a ground-source heat pump. In: Renewable energy resources and a greener future, VIII-11-1. Shenzhen, China: Texas A & M University; 2006.

[66] Hayrullin A, Haibullina A, Sinyavin A. Insulation thermal conductivity heating networks during transportation thermal energy under dry and moisturizing condition: a comparative study of the guarded hot plate and guarded hot pipe method. Transp Res Procedia 2022;63:1074–80. http://dx.doi.org/10.1016/j.trpro.2022.06.109.
[67] McPherson M, Karney B. A scenario based approach to designing electricity grids with high variable renewable energy penetrations in Ontario, Canada: Development and application of the SILVER model. Energy 2017;138:185–96. http://dx.doi.org/10.1016/j.energy.2017.07.027.
[68] Kotzur L, Markewitz P, Robinius M, Stolten D. Time series aggregation for energy system design: Modeling seasonal storage. Appl Energy 2018;213:123–35. http://dx.doi.org/10.1016/j.apenergy.2018.01.023.
[69] van der Heijde B, Vandermeulen A, Salenbien R, Helsen L. Representative days selection for district energy system optimisation: A solar district heating system with seasonal storage. Appl Energy 2019;248:79–94. http://dx.doi.org/10.1016/j.apenergy.2019.04.030.
[70] Gabrielli P, Gazzani M, Martelli E, Mazzotti M. Optimal design of multi-energy systems with seasonal storage. Appl Energy 2018;219:408–24. http://dx.doi.org/10.1016/j.apenergy.2017.07.142.
[71] Wirtz M, Hahn M, Schreiber T, Müller D. Design optimization of multi-energy systems using mixed-integer linear programming: Which model complexity and level of detail is sufficient? Energy Convers Manage 2021;240:114249. http://dx.doi.org/10.1016/j.enconman.2021.114249.
[72] Pfenninger S, Staffell I. Long-term patterns of European PV output using 30 years of validated hourly reanalysis and satellite data. Energy 2016;114:1251–65. http://dx.doi.org/10.1016/j.energy.2016.08.060.
[73] Amirmadhi J, Abeysekera M, Wu J. Modelling of electrical-thermal-hydraulic system interdependencies in 5th generation district heating and cooling networks. In: Volume 23: Sustainable energy solutions for a post-COVID recovery towards a better future: Part VI. 2022, http://dx.doi.org/10.46855/energy-proceedings-9460, preprint.
[74] Abugabbara M, Lindhe J. A novel method for designing fifth-generation district heating and cooling systems. E3S Web Conf 2021;246:09001. http://dx.doi.org/10.1051/e3sconf/202124609001.
[75] Yang T, Liu W, Kramer GJ, Sun Q. Seasonal thermal energy storage: A techno-economic literature review. Renew Sustain Energy Rev 2021;139:110732. http://dx.doi.org/10.1016/j.rser.2021.110732.
[76] Wirtz M. Storages in 5GDHC networks: Benefits, planning, calculation - nPro, https://www.npro.energy/main/en/5gdhc-networks/storages-5gdhc-networks.
[77] Wirtz M. nPro: A web-based planning tool for designing district energy systems and thermal networks. Energy 2023;268:126575. http://dx.doi.org/10.1016/j.energy.2022.126575.
[78] Wilson E. Commercial and Residential Hourly Load Profiles for all TMY3 Locations in the United States. 2014, http://dx.doi.org/10.25984/1788456.
[79] Rockenbaugh C, Dean J, Lovullo D, Lisell L, Barker G, Hanckock E, et al. High performance flat plate solar thermal collector evaluation. Tech. rep. NREL/TP-7A40-66215, Golden, CO (United States): National Renewable Energy Lab. (NREL); 2016, http://dx.doi.org/10.2172/1326887.
[80] Hillel D. Introduction to soil physics. New York, NY, USA: Academic Press; 1982.
[81] Ruhnau O, Hirth L, Praktiknjo A. Time series of heat demand and heat pump efficiency for energy system modeling. Sci Data 2019;6(1):189. http://dx.doi.org/10.1038/s41597-019-0199-y, number: 1 Publisher: Nature Publishing Group..
[82] Buffa S, Soppelsa A, Pipiciello M, Henze G, Fedrizzi R. Fifth-generation district heating and cooling substations: Demand response with artificial neural network-based model predictive control. Energies 2020;13(17). http://dx.doi.org/10.3390/en13174339.
[83] Wirtz M, Kivilip L, Remmen P, Müller D. Quantifying demand balancing in bidirectional low temperature networks. Energy Build 2020;224:110245. http://dx.doi.org/10.1016/j.enbuild.2020.110245.
[84] Wirtz M, Heleno M, Romberg H, Schreiber T, Müller D. Multi-period design optimization for a 5th generation district heating and cooling network. Energy Build 2023;284:112858. http://dx.doi.org/10.1016/j.enbuild.2023.112858.
[85] Zarin Pass R, Wetter M, Piette M. A thermodynamic analysis of a novel bidirectional district heating and cooling network. Energy 2018;144:20–30. http://dx.doi.org/10.1016/j.energy.2017.11.122.
[86] Zhang Y, Johansson P, Kalagasidis AS. Quantification of overlapping heating and cooling demand for the feasibility assessment of bi-directional systems over europe. Energy Build 2023;294:113244. http://dx.doi.org/10.1016/j.enbuild.2023.113244.
[87] Miri M, Saffari M, Arjmand R, McPherson M. Integrated models in action: Analyzing flexibility in the Canadian power system toward a zero-emission future. Energy 2022;261:125181. http://dx.doi.org/10.1016/j.energy.2022.125181.